Rochester Institute of Technology

RIT Digital Institutional Repository

7-22-2024

Combined Virtual Reality and Mechanical Balance Platform System with Induced Visual Roll

Shkenca Demiri
sd4975@rit.edu

Follow this and additional works at: https://repository.rit.edu/theses

RIT

**Combined Virtual Reality and Mechanical Balance Platform
System with Induced Visual Roll**

by

Shkenca Demiri

A Thesis Submitted in Partial Fulfillment of the Requirements for the

Degree of Master of Science in Mechanical Engineering

Department of Mechanical Engineering

Kate Gleason College of Engineering

Advisor: Dr. Kathleen Lamkin-Kennard

Thesis Committee:

Dr. Michael Schertzer

Dr. Isaac Perez-Raya

Dr. Sarilyn Ivancic, Department Representative

Rochester Institute of Technology

Rochester, NY

July 22, 2024

ABSTRACT

Balance impairments are a common and widespread concern in human health. Acquired through genetics, aging, illness, or prolonged exposure to different environments such as travel by sea or travel in outer space; balance impairments pose significant challenges to those affected. Traditionally, balance studies have been largely qualitative. However, technological advancements have allowed for new methodologies to be developed for analyzing postural sway in a quantitative manner. In this thesis, custom force plate technology, an advanced inertial motion unit (IMU) motion capture system, and a mechanical motion platform, in tandem with a gamification system, were integrated to collect and analyze quantitative data to offer valuable insights into an individual's sway characteristics and postural control mechanisms. Results from the study validate the use of the system to strengthen its feasibility as a valuable tool for facilitating larger human subject studies. Identification of pertinent data for conducting balance assessments was explored, and a protocol for utilizing the system to gather and display this data was established. Center of Pressure (COP), Center of Mass (COM), and body segment data were used to analyze movement in mediolateral (ML) and anterior-posterior (AP) directions to help answer the overall question: How can virtual reality, motion capture, and a mechanical platform system be integrated to quantitatively assess changes in human balance responses? The versatility of the system was leveraged to have a subject perform tasks under different visual conditions and platform positions. Methods used in this thesis for collection and presentation of data showed that the gamification system is able to detect changes in postural sway, which is vital to being able to conduct larger group studies. The findings underscore the system's potential to be used for biomechanical analysis, medical rehabilitation and balance training.

Table of Contents

LIST OF FIGURES

LIST OF TABLES

NOMENCLATURE

COM = Center of Mass

COP = Center of Pressure

AP = Anterior-Posterior

ML = Mediolateral

BASE = Balance Apparatus for Sensorimotor Evaluation

SVV = Subject Visual Vertical

SVH = Subject Visual Horizontal

CDP = Computerized Dynamic Posturography

1.0 MOTIVATION

Balance impairment is common among many populations all over the world. Quite often, increased variability in postural sway can be induced when visual changes occur, stemming from a mismatch between what people are seeing not matching up with what they are feeling. As a result, individuals who experience these feelings have an increased fall risk, which can result in severe injury. In order to analyze and rehabilitate those who experience balance impairments, visual displays, in combination with mechanical platforms that are equipped with force plates, are found in some medical offices to both create different balance scenarios and gather balance data. The systems can be used to induce illusions of self-motion to practice improving balance in a safe manner. Recently, medical experts have been exploring the use of head-mounted virtual reality displays as a way to provide a viable alternative intervention for fall prevention rehabilitation. Virtual reality can allow for more easily manipulated and more realistic looking visual experiences as compared to prior methods that utilized large screen displays.

Studies have been done that focused on the use of virtual reality to help rehabilitate those with balance impairments, however, there have been limited studies done that looked at the effects of altered visual conditions on human biomechanical responses. Additionally, limitations of these studies often include limited degrees of freedom for both viewing fields and restrictions on human body positioning. For those studies that have been conducted, data has typically been gathered and analyzed only in one plane of movement. Data has been gathered either by using subject visual vertical (SVV) or subject visual horizontal (SVH) tests to evaluate the subject's perception of orientation, or by using diodes placed on only one plane of a person's body to visually track movement.

Inertial motion capture systems, such as the Xsens Awinda system (Xsens Technologies BV, Enschede), offer a compelling solution for capturing motion in three dimensions due to several advantageous features. A key advantage lies in their ability to operate without reliance on external reference, such as GPS or external cameras, making them suitable for use in a more portable manner. By capturing motion in 3D rather than just 2D, the question as to how the additional dimensionality can yield a more comprehensive understanding of a subject's

movement can be studied in more depth. The combination of using force plate, virtual reality, mechanical platform technology in tandem to study postural control biomechanical effects of such systems will help to pave the way for more advanced balance rehabilitation systems.

2.0 LITERATURE REVIEW

The field of virtual reality has grown at a quick pace in recent years. Its applications have moved from being used for purely entertainment purposes to being used for situational field training and medical rehabilitation. Due to the advancements of such technology, people have been able to leverage using a combination of virtual movement and mechanical movement to better study and rehabilitate biomechanical effects of individuals experiencing balance impairments. The following presents a summary of relevant scholarly work in this field of research within current literature that this research will further develop.

Vestibular, sensorimotor, and proprioceptive senses are all integral to human balance [1]. The senses can be altered situationally, whether it be due to physical trauma, disease, aging, or disrupted gravitational and visual experiences. Information gathered from spaceflight and related research suggests that the reduction in physical load might lead to less reliance on proprioception. This adaptation plays a significant change in the role of balance issues experienced upon return from space [2]. A major challenge presented to those experiencing balance impairments is fall risk. This is attributed to the fact that those who are impaired typically experience adverse effects in their gait and have trouble safely completing tasks that require standing or moving [3]. Rehabilitation of gait disorders is often based on conventional treadmill training or other standard physical therapies.

Balance control depends on the central nervous system at many levels. Some studies have shown that by using virtual environments, the cortical and sub-cortical regions of the brain are activated [49, 50]. By introducing virtual reality based training, a user's visual experience can be altered in a multitude of ways, allowing for clinicians to induce a wide range of visual motion situations. Additionally, increased levels of interactivity and having the ability to create more interesting and appealing visual imagery during training can improve an individual's motion to train [4]. Virtual reality (VR) technology enables users to be immersed in an environment where audio, visual, and haptic feedback can be experienced in a three-dimensional visual space. Interactive experiences created by virtual reality technology allow a user to concentrate on autonomy and interaction. Berra [47]

suggested that patients may be able to work on skills that allow them to work independently, which may improve quality of life, using VR technology. Quinliavn et al. [48] showed that head-mounted displays could play a role as novel research tools for investigations regarding normal and abnormal patterns of movement. In the study, a VR system (Oculus Rift DK2) was used by 40 healthy adults in order to present visual stimulus and gather data on head turn movements. The work represented the first time that the Posner cueing effect had been observed in the onset of head movement in humans, as it was found that there was a relationship between head movement onset and saccade onset.

By combining virtual reality head mounted displays with a mechanical platform, different positional situations can be further induced in a manner that is both visual and physical [1]. To analyze the effects of using these systems on factors such as balance, biomechanical analysis is typically done using a variety of different data gathering methods. Balance ability is significantly related to the position and velocity of the entire body's center of mass (COM). As a result, the COM has been used as a good indicator of postural stability. Tracking COM position is commonly done using force plates implanted into a surface that a subject would be standing on or by using motion capture devices, such as Kinect sensors or a Vicon motion capture system [5]. The COM of the body is calculated using a weighted sum of the COM position of each body segment. To estimate the COM, segmentation techniques that track positioning of individual body segments must be used. This is usually done using motion capture systems, which can be either marker based or markerless. Marker based motion capture systems, however, do have numerous faults, including not being portable and that individual markers must remain visible to cameras at all times. Inertial motion capture systems provide an alternative way to capture motion in 3D while avoiding the pitfalls of having to use them in a laboratory setting. Additionally, receiving measurements from inertial sensors does not rely on having to be restricted to specific orientations to ensure camera viewing. Using these in combination with a force plate can provide a more detailed picture of what motion is occurring in an individual over time.

Measuring postural sway can be used to assess changes in balance over time. Sway measurements have been used in post-traumatic brain injury studies [6], in older adults

[7,8] and in those with neurological disorders. Currently, the most commonly used technological systems include computerized dynamic posturography (CDP) and force plates, which measure the center of pressure (COP) of a subject. Studies have shown that COP can be correlated with poor balance and fall risk. [9].

 Although several studies have been done on the combined use of mechanical systems with virtual reality, the types of visuals being shown and their effects on human balance remain to be explored. Particularly, there are gaps in the literature pertaining to the more specific study of the effects of a subject experiencing visual roll. The relationship between balance and visual roll is crucial, as human perception of balance can be heavily influenced by visual stimuli, particularly those that induce a sense of motion and disorientation. Circular vection, also known as visual roll, is the perceptual illusion of seeing a rolling motion in the visual field while being physically stationary. Humans typically feel a compelling illusion of self-motion when being introduced to this type of visual stimulus.

Timing and kinematic alterations of body movement are typically affected when a subject experiences visual roll motion. A study by Dvorkin et al [10] demonstrated how the presence of visual roll can lead to changes in the ratio of trajectory types and notably extended pauses when reaching outward. The study concluded that both the temporal and spatial kinematics of that reaching movement were affected.

Tanahashi et al [11] completed a study in which observers completed experimental conditions that matched four different combinations of rotation direction associated with the visual roll stimulus. This included two different visual stimulus patterns. The visual roll motion had a velocity maintained at 60 deg/sec, and the subjects maintained an upright position with feet together and arms relaxed at their side. The postural movements, however, were only measured using a force platform in conjunction with a head position sensor placed on a helmet worn by the subject. Although this study showed that visual stimulus has an affect on postural control, it was restricted to having measurements of movement taken only from center of pressure and head position data, disregarding movements at other parts of the body.

When not using virtual reality, impact of roll visuals on both postural sway and the SVV has typically been studied using mechanical devices as well as non-head-mounted electronic displays or projections. The devices were limited by their tendency to emit and reflect light from the edges of their screens or corners of the room, which provides a fixed Earth-based reference of verticality. Lubek et al [12] completed a study in which subjects were exposed to a visual dot pattern that either remained unmoving, or was rotated in a roll motion. This visual was shown in two different conditions, either being surrounded by an Earth-fixed reference frame, or not. Although this was not done using virtual reality, the subjects viewed the visual stimulus on a 40-inch TV screen in high-definition resolution. The edges of the screen were covered by a low reflective removable cardboard cover, which left a circular viewing area. The study took place in a dark environment. The subjects also wore neutral density goggles that allowed a 1% passage of light. The combination of these two precautions represented a "No Frame" condition. The "Frame" condition consisted of a random dot pattern surrounded by a yellow square frame and the circular cover removed. During the separate trials of the experiment, the subjects were asked to adjust a rod to match their perceived SVV. The results of the study showed that having an Earth-fixed reference frame that surrounded the rotating pattern resulted in less variability and less lean during upright standing, as well as more accurate SVV estimates. The findings were consistent with results from Tanahashi et al., as well as other earlier studies, which showed that visual roll motion resulted in a notable shift in the SVV away from its alignment with the Earth's vertical.
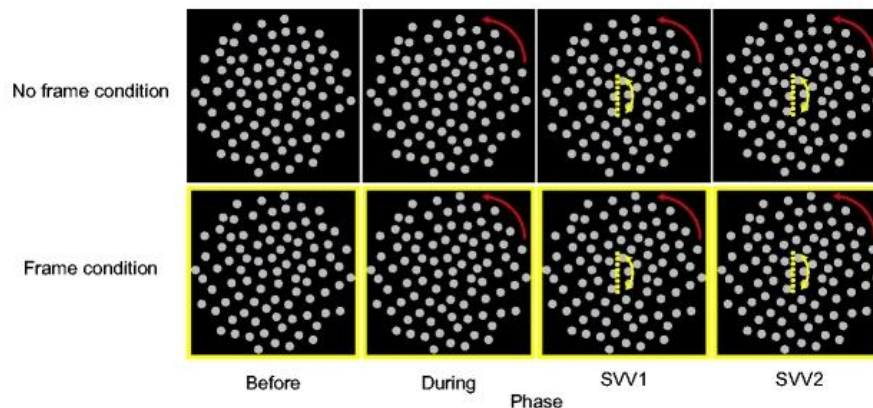
Figure 1: Graphical illustration of the experimental setup from Lubeck et al. [12]

A widely used method to measure the effect of circular vection on visual vestibular perceptions is to have an individual sit and instruct them to adjust their subjective visual vertical or subjective visual horizontal based on whole body tilt. A study by Wang et al. [13] showed that visually induced circular vection differs for supine and upright participants. The study examined effects of viewing positions while watching random dots rotating at different angular velocities for 30 seconds (92×60 degree view field rotating at 2, 4, 8, 16, 32, 64 deg/s). In this study, it was found that the onset of roll circular vection occurred much earlier in subjects situated in upright positions, and the roll circular vection durations were typically lengthier than those situated in laying down positions at lower velocities.

A study by Ward et al. [14] required a human subject to look at a roll visual, but was restrictive in having the subjects constrained using a four-point safety belt and having their head be constrained to a "straight ahead" position.
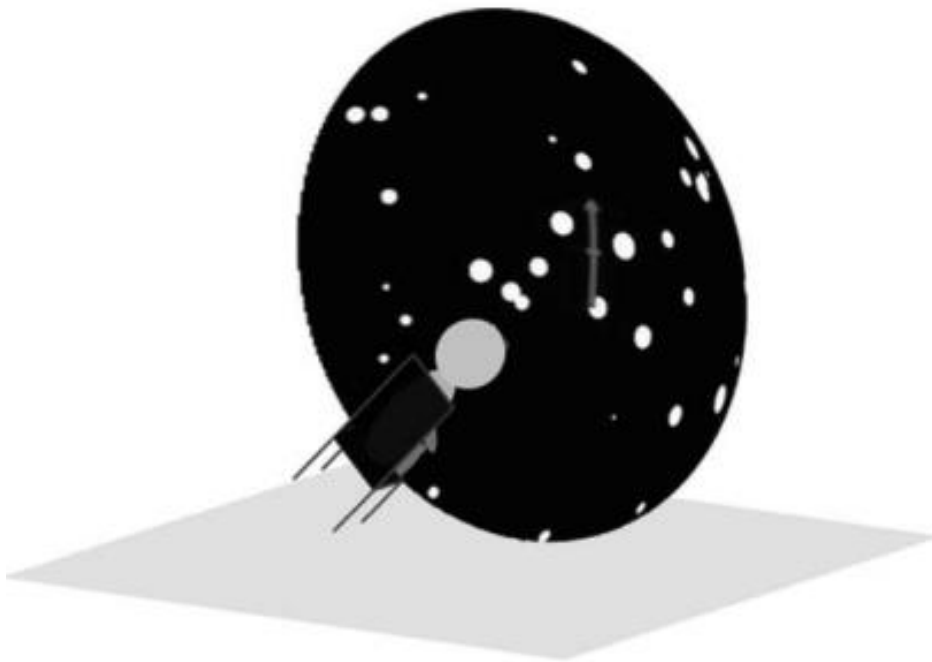
Figure 2: Graphical illustration of the experimental setup from Ward et al. [14]

Cleworth et al. [15] conducted a study on the impact of roll circular vection on roll tilt postural responses, as well as on the subjective postural horizontal. The study used a head mounted display to investigate how dynamic visual cues, shown as circular vection, influenced postural responses as well as the how the subject perceived the horizontal both during and after tilting of the support surface. The study was limited however to a singular plane, as the support surface was only on a pivot board that allowed for tilt in only one direction. Additionally, data was collected using light emitting diode markers mounted to the head trunk and pelvis, only providing a 2D view of human motion.
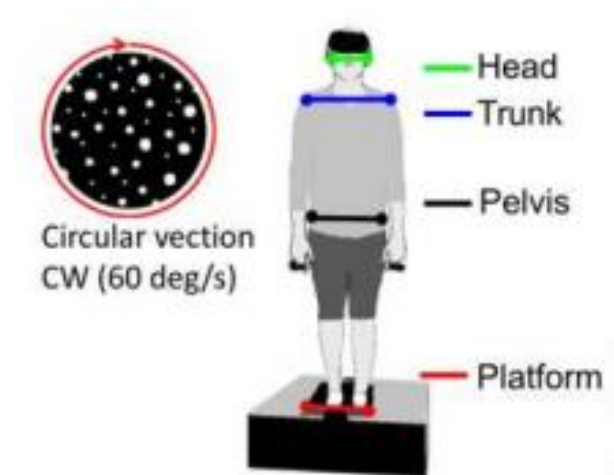
Figure 3: Graphical illustration of the experimental setup from Cleworth et al. [15]

King et al. [16] conducted a study exploring how the upright postural control system adapts dynamically to internal and external disturbances. The purpose of the study was to assess how visual information and support surface angles impact time scales involved in maintaining upright stance. Thirteen young adults participated in standing tasks taking place on a surface that was either slanted or level, with their eyes being either opened or closed. The results indicated that sway was more pronounced in slanted conditions as compared to the level surface condition when vision was removed. It was also found that there was an increase in irregularity in postural sway on tilted surfaces, and the complexity of the COP increased in the absence of visual input. Generally, the range of postural adaptability was similar across the manipulations, which suggests that there are boundaries to the extent of changes in the dynamics of the COP.

Several methods have been used to assess the performance of standing balance. In clinical settings, balance is usually gauged by the length of time a subject can maintain stability without falling or altering their base of support by moving their feet. Another way to evaluate performance is by the degree of postural sway exhibited. There are several ways to measure postural sway, including tracking movement of center of pressure (COP) and center of mass (COM). The COP is the point where the vertical ground reaction vector intersects the support surface and is different from the COM, which calculates the position of the total mass of all body segments in space. When considering an inverted pendulum model under quiet standing conditions, movement and variability of movement have been employed as indicators of postural stability [17,18]. To improve understanding of early changes in standing balance, other metrics have been explored. The frequency-domain characteristics of a system offer another way to analyze changes in the balance system. From a systems theory perspective, balance is maintained through an interplay of several subsystems. Each subsystem has uniquely characterized frequency bands. If a subsystem fails, there will be a change in its characteristic frequency band [19]. Power spectrum density analysis is a tool frequently used in literature to conduct studies pertaining to this. Studies have demonstrated that the spectral frequency characteristics of a balance control system may be beneficial in detecting minor system changes. For instance, Mauritz et al. [20] showed the frequency spectrum of individuals that had cerebellar ataxia showed unusual frequency peaks at 0.7 and 3.0 Hz.

To estimate spectral density, Welch's method can be used. Welch's method is used typically for analyzing what the power of a signal is different frequencies [53]. The method is a step up from a traditional periodogram spectrum estimation method as it decreases the amount of noise in the estimated power spectra. However, it is important to note that doing this can come at the cost of a tradeoff in frequency resolution. To reduce variance of a periodogram using this technique, a time series is divided into overlapping segments, thereby calculating a modified periodogram for the individual segments. Then, the method involves averaging the estimates to provide for a PSD estimate. Usually, there is also a window function that is applied to the segments.

Cherng et al. [21] believed that there was limited information pertaining to the frequency spectrum of the balance control systems of children. They conducted a study for standing balance under six sensory conditions, achieved by crossing three levels of visual factors (eyes opened, eyes closed, and sway referenced vision) along with two levels of foot support, which were either fixed or compliant. The findings showed that when comparing children with adults, there were differences in the spectral frequencies. For some of the conditions, it was observed that children had higher median spectral frequencies. This suggested that they might have not completely established an ankle strategy for maintenance of balance. However, they were still able to achieve the same level of ability of using vision as reference for maintaining standing balance.

Postural control is generally considered to have two critical modes of control. The modes of control consist of a single-joint, inverted pendulum "ankle strategy" and a two-joint double-pendulum "hip strategy" [22,23,24]. The ankle and hip strategies are characterized by their individual rotations. When a subject is standing quietly or experiencing slight perturbations, the nervous system resorts to using the single-joint ankle strategy, and active control of COM motion is resultant mostly from the torque of the ankle [25]. In situations where there are significant shifts in support surface movements, the body tends to employ the hip strategy. It is widely believed that these fundamental patterns are chosen from a collection of motor programs which originate from advanced neural strategies and are executed by intricate sensorimotor control processes to effectively counterbalance physical attributes of perturbation [26]. Zhang et al. [27] demonstrated that the patterns of the leg and trunk during a quiet stance vary in response to different sensory inputs.

Creath et al. [28] conducted a study to explore how dynamics between body segments adjusted to sinusoidal platform movements, both with and without extra somatosensory input through fingertip touch contact. The study was able to use PSD analysis to gather results that suggested that balance instability of bilateral vestibular loss patients comes from high variability of trunk movement instead of leg movement.

Studies have shown that a subject standing erect in a positive gravitational field can sense a shift in what they perceive to be vertical after they view a roll visual. The perception is thought to

come from the interaction between the visual and vestibular systems. The otolith signal and visual system's motion signal integrate, causing the subject to feel like they are being tilted to the side opposite of the direction of the visual motion. The normal biomechanical response to compensate for this is to lean towards the direction of the visual motion. Keshner et al. [29] conducted a study in order analyze the effect of an immersive dynamic visual field on segmental postural stabilization, and examined resulting power spectrums, finding that changes in visual surrounding generated postural reorganization.

The manner in which the vestibular sensory system contributes to the coordination of ankle and hip postural strategies is not well understood. This is partially attributed to the lack of research studies conducted on looking at balance in both the AP and ML plane, and lack of the equipment and ability to realistically manipulate different balance scenarios through platform perturbations and different visual scenarios.

Numerous studies have investigated the effects of visual roll without leveraging virtual reality, which, while informative, may not offer the optimal immersive experience. On the other hand, existing virtual reality studies have often constrained subjects to a seated position, limiting natural range of motion. Moreover, biomechanical data collection methods in these studies have been somewhat rudimentary, focusing on singular planes of motion and utilizing sensors tracked exclusively within those planes. This thesis aims to address these limitations by integrating virtual reality with a mechanical platform system. Employing an inertial motion capture system, this research endeavors to comprehensively analyze the biomechanics involved when subjects experience visual roll. The approach is designed to provide a more realistic and less restrictive environment for both movement and data capture, contributing to a more nuanced understanding of the phenomenon, all while utilizing a custom gamification system crafted and constructed by students at RIT.

3.0 RESEARCH QUESTION

The thesis project seeks to answer the following research question: How can virtual reality, motion capture, and a mechanical platform system be integrated to quantitatively assess changes in human balance responses?

4.0 OBJECTIVES OF THE PROPOSED WORK

The following objectives and associated subtasks will be undertaken as part of the thesis work:

1. **Validate individual system components and create protocol to be used for gamification system:** Validate and assess custom motion platform's ability to achieve position reproducibility. Validate the custom force plate's ability to gather accurate measurements. Validate and utilize an inertial motion capture system to accurately track a subject's position and orientation over time in response to changes in platform and visual conditions.

2. **Create and implement a visual to be viewed in a virtual reality headset that can induce changes in postural stability:** Select a virtual reality headset capable of allowing visuals to be played without distortion. Prototype visual to be viewed using a head mounted display by a human subject. Create "in game" metrics that can provide quantitative data to assess balance.

3. **Create methods of data capture pertinent to balance studies**: Identify quantitative parameters that can be used from each of the system components to analyze postural stability. Show how data obtained simultaneously from disconnected systems could be used in tandem to obtain information about balance. Condense and interpret the extensive data sets obtained from the system components to present them in an insightful way.

5.0 METHODOLOGY

5.1 Subsystem Validation

The training system can be broken down into several subsystems. The support rig consists of the frame and motion floor (actuators), the force plate embedded into the motion floor, and the software that was developed to create the Virtual Reality game (roll visual). The Xsens Awinda was used as the motion capture system in this study. The validation of these subsystems is key for successful implementation of using the system to conduct balance studies.

5.2 BASE

The novelty of the system is that it not only allows fixed rotation about any axis, it can also generate oscillatory actions. Dynamic testing over extended periods of time can be done. The angles at which the platform can be situated can be moved at various speeds.

The virtual reality gamification system previously developed at RIT was created by a Multidisciplinary Senior Design (MSD) team, but not validated, particularly for balance studies. The mechanical motion platform, called the Balance Apparatus for Sensorimotor Evaluation (BASE), was originally designed to work in tandem with a virtual reality display visual. The frame of the BASE is made out of 11 gauge steel rectangular tube with 12 gauge flat brackets. It is 6ft in width, 6ft in length, and 8 ft in height. An anchor strap is looped around the center of the top of the frame to support a subject using a 4 to 6 ft adjustable static strap. The user first is required to put on a safety harness, and then clip themself into the above safety strap. The belt locks once immediate sharp movement is detected, much like a seatbelt, so the user can be prevented from falling. The structure of the BASE is designed to safely withstand a 600 lb force. As shown in Figure 4, the motion platform of the base is supported by a U-Joint to allow for two degrees of freedom in motion.

Figure 4: U-joint under center of BASE platform.

Two actuators are able to tilt the platform of the base 20 degrees in all four directions (forward tilt, backward tilt, left tilt, and right tilt). The actuators, shown in Figure 5, contain Allen-Bradley PLC and servo drivers (Tolomatic, Hamel MN). They also contain Tolomatic linear actuators driven by Allen-Bradley servo motors that have a max force of 500 lbf X 2, max stroke of 24in, and max speed 38in/sec.

Figure 5: Image of one actuator.

The specifications for the ranges of the actuators are shown in Table 1. The input value range represents the minimum and maximum values, as defined by the manufacturer, that the user of the actuators can input in order to control the rates of speed, acceleration, and position.

	Input Value Range	Corresponding Units
Right Speed	1-30,000	0.01 mm/sec
Right Acceleration	500-90,000	0.01mm/sec^2
Right Position	-25,000-0	0.01 mm
Left Speed	1-30,000	0.01 mm/sec
Left Acceleration	500-90,000	0.01mm/sec^2
Left Position	-25,000-0	0.01 mm

Table 1: Range values and corresponding units for actuators.

In order to control the actuators to move the BASE platform, the specifications from Table 1 can be input into Visual Studio Code. The home position is that in which the platform is completely level. The BASE platform should always be put into its home position when being turned on prior to testing human subjects. In order to control the movement of the base, the following line of code represents how information should be input. Any values that fall within the Input Value Range of values in Table 1 above, are acceptable inputs. Only integer values should be input.

```
actuator_control_test.actuator_home(3)
def actuator_move(speed_right: int, acc_right: int, pos_right: int, speed_left: int, acc_left: int,
pos_left: int):
```

Figure 6: Snippet of code to control actuators from VS code.

The repeatability and reproducibility of actions and related motion input of the platform of the system in response to different inputs was verified. The maximum angles of tilt for the BASE system were verified in each direction physically using a digital level (Klein Tools Digital Angle-Gauge and Level, Lincolnshire IL). The digital level has an angle capability of 180 degrees. The accuracy is +/- 0.1 degrees for all angles falling in the 0-1, 89-91, 179-180 degree ranges, and +/- 0.2 degrees at all other angles. Figure 7 shows an example of how the level was used to measure the angle at which the platform was moved to. For the forward and backward tilt angle measurement tests, the level was used to take three measurements on the platform. One measurement was taken at the center of the force plate, one taken on the left outer edge of the platform, and one on the right outer edge of the platform. The measurements were done to ensure that the entire plane of the platform was at the same angle, and that both actuators consistently moved to the correct positions. For left and right tilt angle measurement tests, the same process was followed, however measurements were taken on the back and front edges of the BASE platform instead of left and right.
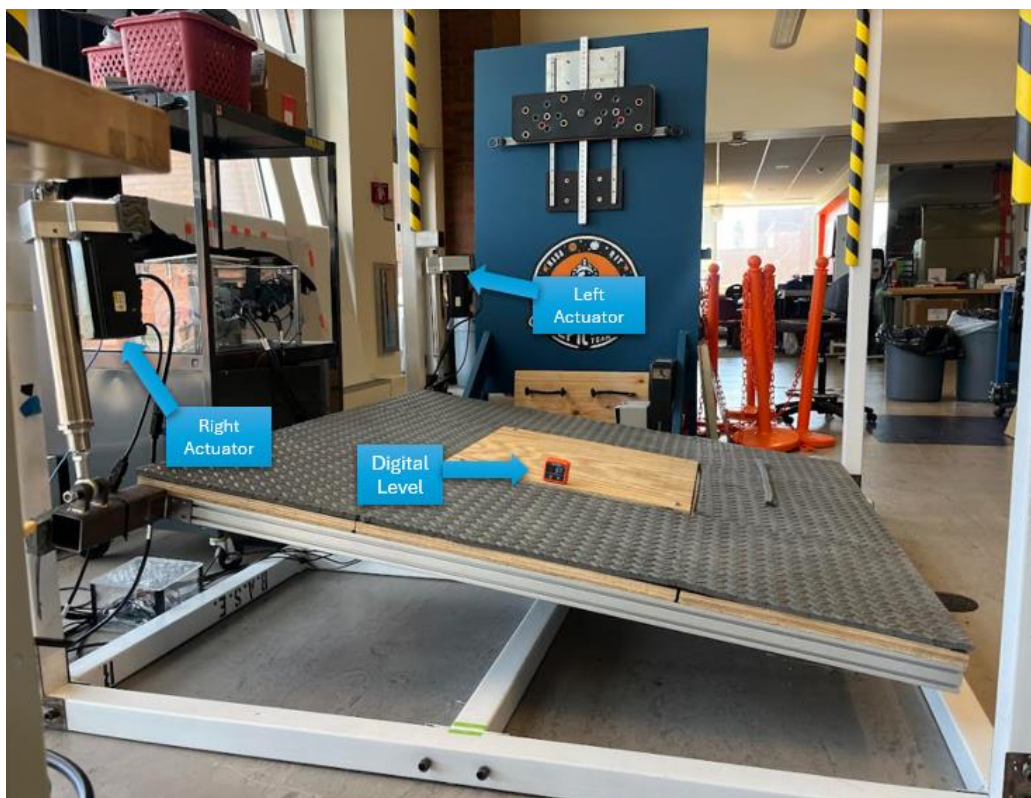
Figure 7: Image showing the BASE tilted at an 8.7 degree forward angle with the digital level placed on top of the force plate.

The ability to control the angles of tilt and reproduce them consistently was also confirmed. Tables 2 and 3 show the trial results recorded for each direction of tilt, as well as resulting percentages of error. The method was done for forward, backward, left, and right tilt directions. The tables below show examples of the platform angle readings in different configurations.

The following inputs were used to test forward tilt at two separate angles. For the first position (position #1), the input values were 1000 for the velocity of the right actuator (speed_right), 500 for the acceleration of the right actuator (acc_right), -4000 for the position of the actuator (pos_right), 1000 for the speed of the left actuator (speed_left), 500 for the acceleration of the left actuator (acc_left), -4000 for the position of the left actuator (pos_left). For the second position (position #2) the input values were 1000 for the velocity of the right actuator (speed_right), 500 for the acceleration of the right actuator (acc_right), -2000 for the position of the actuator (pos_right), 1000 for the speed of the left actuator (speed_left), 500 for the acceleration of the left actuator (acc_left), -2000 for the position of the left actuator (pos_left).

Trial #	Center Reading (Deg)	Left Edge Reading (Deg)	Right Edge Reading (Deg)	Average
1	7.7	7.8	7.7	7.73
2	7.7	7.7	7.7	7.70
3	7.7	7.8	7.7	7.73
4	7.8	7.7	7.8	7.77
5	7.7	7.8	7.7	7.73

Table 2: Platform movement angles in response to forward tilt inputs, position #1.

Trial #	Center Reading (Deg)	Left Edge Reading (Deg)	Right Edge Reading (Deg)	Average
1	9.7	9.6	9.5	9.60
2	9.5	9.7	9.5	9.57
3	9.7	9.6	9.7	9.60
4	9.5	9.5	9.6	9.67
5	9.7	9.7	9.5	9.63

Table 3: Platform movement angles in response to forward tilt inputs, position #2.

The total average reading across all trials for the forward tilt position #1 was 7.7 degrees. The total average reading across all trials for the forward tilt position #2 was 9.6 degrees.
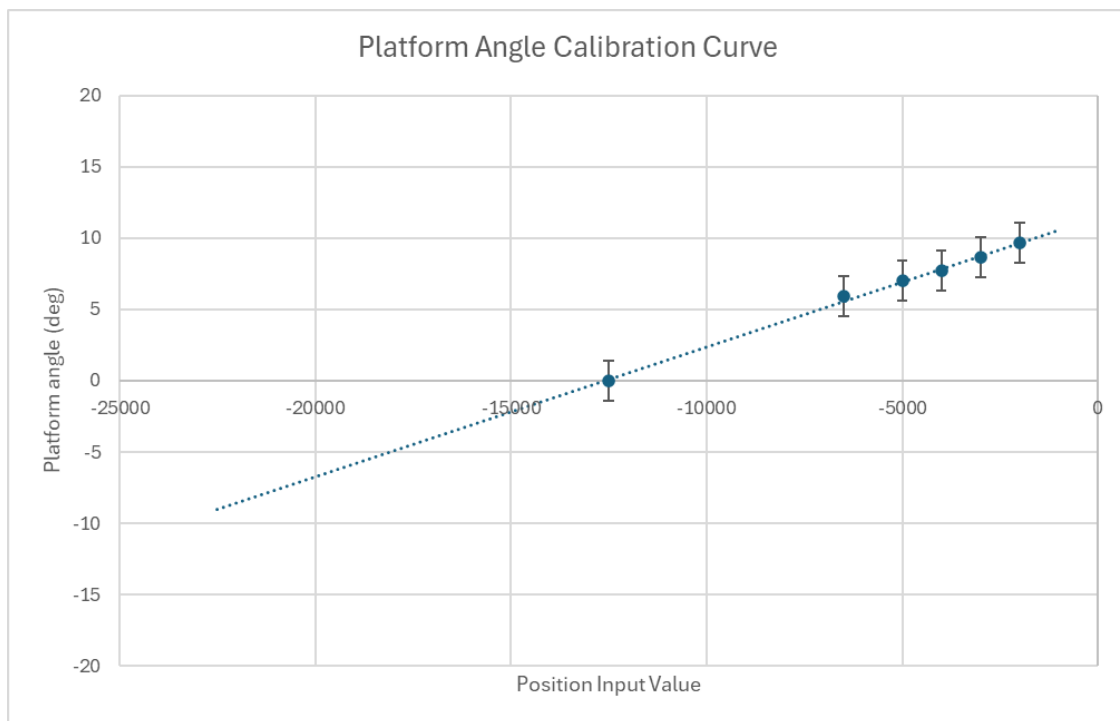
Figure 8: Graph of calibration curve for forward and backward tilt of the BASE platform.

Figure 8 shows the results of the position input values relative to the measured platform angle of the BASE. It is important to note that negative angles are considered to be the platform tilting in the backward direction, and positive angles indicate that the platform is tilted in the forward position. Also, as shown in the graph, the point of intersection of the trendline and the x-axis is where the level position of the platform is located. According to the value given by the manufacturer, -12500 is the home position input value. When measured with the digital level, when both actuators are set to -12500, the platform consistently produces angles that result in an average of a zero degree tilt.

5.3 Force Plate

Several methods exist for the assessment of balance. In clinical settings, balance is typically assessed through qualitative tests. In laboratory settings, depending on available instrumentation, factors of balance can be more quantitatively analyzed. To date, force platforms are a common tool used for data collection. The BASE incorporates a uniaxial force plate into the center of its standing platform. The top of the force plate is designed to be flush and parallel with the top of the platform. The force plate is constructed from a thin rigid plywood board and equipped with four S-Type TAS501 load cells (SparkFun Electronics, Niwot CO). Each of the load cells is positioned at a corner of the board. The initial design of the system consisted of a steel plate with 80lb-in springs beneath it to counteract deflection of the subject standing on it. However, this design was limited, as the steel plate and springs caused significant deflection of warping. This not only led to inconsistent load cell readings, but it also posed a risk to safety for subjects standing on the platform as their feet could get caught at the deflection point between the surface of the platform and the depth of the well housing the load cells.

Figure 9: Image of force plate wooden board with tape measure showing length of 24 inches (609.6mm). The arrow points to the origin of the coordinate system aligning with stabilogram centers.

In order to rectify these issues, the force plate was redesigned using rigid plywood cut to precise dimensions to fit the well. The new design eliminated the need for additional springs to prevent deflection due to the inherent rigidity, which helps to ensure accurate readings from the load cells. Each one of the load cells is equipped with four strain gauges arranged in a Wheatstone bridge configuration, and are capable of converting a maximum force of 200 kg into an electrical signal. An HX711 load cell amplifier was used to extract measurable data from the load cells. Each load cell was individually calibrated using a modified Arduino code, based on an example provided by SparkFun Electronics, as shown in Appendix A. The steps for calibration of each individual load cell were as follows. First, the calibration code was verified and uploaded with no masses placed on the load cells. Once readings were displayed, a known 10kg mass was placed on one load cell at a time. While watching the results on the Arduino serial monitor, the "plus" and "minus" buttons of the keyboard were then pressed to adjust the calibration factor so

that the output readings matched the known weight. The process was repeated for each of the four load cells to obtain individual calibration factor values.

The following values were obtained as calibration values for load cells 1,2,3, and 4 respectively: -21350, -20850, -22700, -22700. After the calibration values were obtained, the Arduino code shown in the Appendix B was used to provide scale outputs. Each individual load cell was tested with 5 different masses in order to ensure repeatability of measurements. Some variability, up to 0.1 kg, was observed between measurements. However, the measured errors were within the acceptable range of error given from SparkFun's datasheets for the load cells. CoolTerm (developed by Roger Meier as freeware), a sophisticated serial port data capture tool, was used for real-time data logging to allow for efficient handling of the high-throughput data stream from the Arduino and save data directly to the computer. CoolTerm provides the capability to record data in various formats such as TXT, CSV, or Excel. Saving data in these formats helped facilitate subsequent data processing and analysis, thereby streamlining the data gathering process for analyzing center of pressure (COP) data.

In humans, to maintain balance and upright posture, the simultaneous control of posture in both AP and ML directions is used. The movement of COP in these two directions can provide valuable insights into postural stability of an individual (Rhea et al). In the literature, there is a predominance of studies that were conducted analyzing data from only the AP direction over the ML. The AP direction was done primarily because many daily activities, such as running or walking, primarily involve movements in the sagittal plane (AP direction), making AP sway more significant to these common tasks. Historical precedence was also a factor, as early research and models on postural control often focused on AP sway, which could possibly have influenced the focus on subsequent studies, given that research on biomechanics overall is a relatively very new field. Additional studies including ML sway analysis allows for a more comprehensive understanding of balance. The system and protocol presented in this thesis ensures that ML sway is also analyzed.

COP contains features that allow for characterization of a subject's postural strategies and modifications which provides information that can be useful when analyzing balance [32].

Additionally, analyzing COP positioning has been used to determine motor strategies for fall prevention. COP is the point where plantar ground reaction force is applied. COP characterizes the center point of the entire pressure in the ground-foot surface of contact [33,34]. The ground reaction force is typically measured using a force plate. The COP for this system was calculated as done by Bartlett et al. and Fauzi et al. [30,31]. However, it should be noted that this formula assumes that the forces are acting perpendicular to the force plate and that the force plate is level.

$$COP_X = \frac{L((S2+S4)-(S1+S3))}{2(S1+S2+S3+S4)} \tag{1}$$

$$COP_y = \frac{L((S2+S1)-(S4+S3))}{2(S1+S2+S3+S4)} \tag{2}$$

L = length of the plate (609.6mm)
S1= force in kg on load cell 1
S2= force in kg on load cell 2
S3= force in kg on load cell 3
S4= force in kg on load cell 4
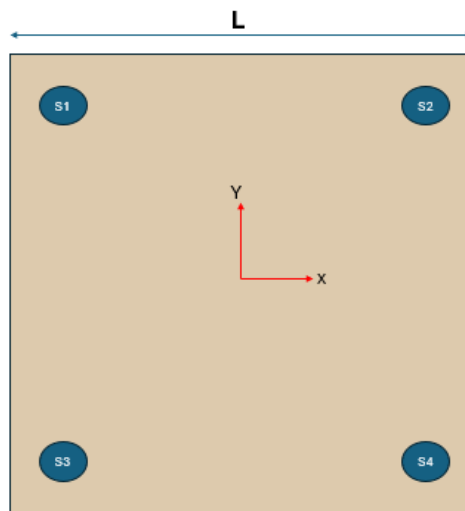
Figure 10: Schematic diagram of force plate.

While the force plate was in the level (no tilt) condition, a subject was asked to stand with their feet at a comfortable shoulder length distance apart as near to the edge of the force plate as they could, at four different locations.
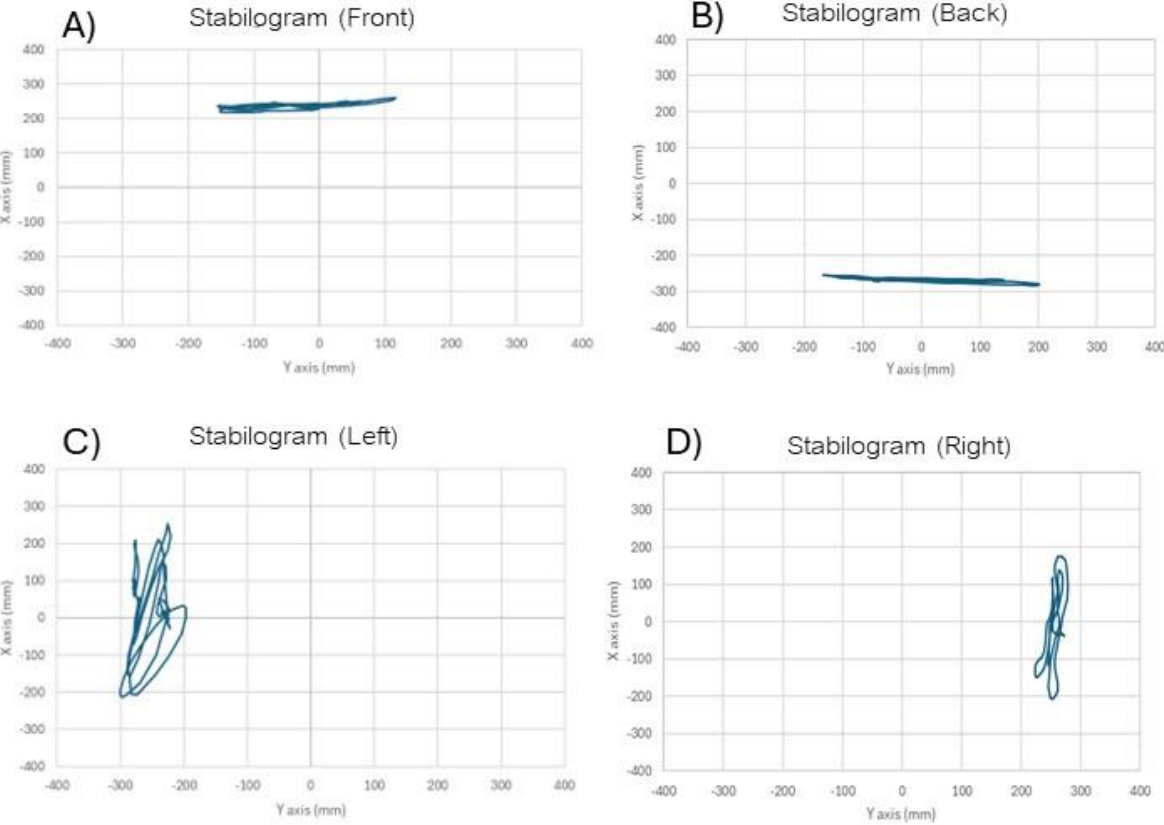
Figure 11: Subplots of stabilograms created from force plate data, graph A is forward position, graph B is backward position, graph C is left position, graph D is right position.
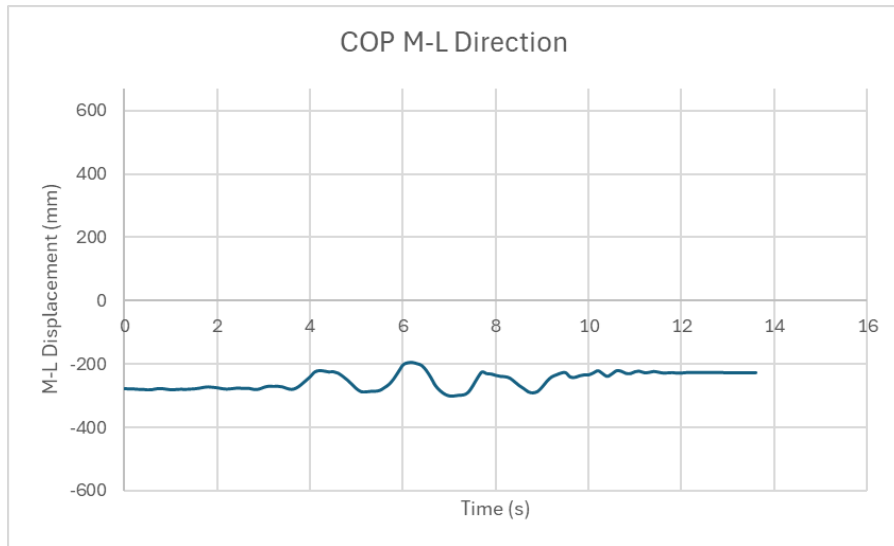
Figure 12: ML displacement time series graph for subplot C.
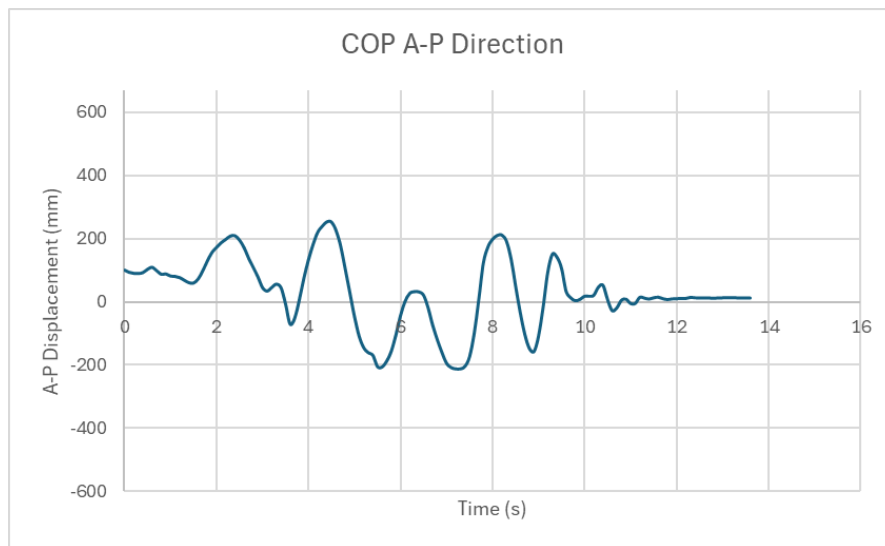
Figure 13: AP displacement time series graph for subplot C.

Figure 11 contains subplots of stabilograms that effectively demonstrate the force plate and MATLAB code proficiency in generating data that accurately corresponds to the COP when the subject is standing positioned on different sides of the force plate. Subplot C is one stabilogram created for when the subject is standing on the left side of the plate. The COP data points are all clustered toward the left side of the plate and the stabilogram shows no stray graphing on the right side of the graph or near the midpoint of y axis, showing a reasonable projection of the path of the COP should someone stand on the left side of the platform. Similar results are consistent

for the rest of the stabilograms and their corresponding directions. Figure 12 is a graph of a time series showing the displacement in the ML direction, measured in millimeters. Figure 13 is another graph of the time series showing the displacement data in the AP direction. It is important to note that the peak-to-peak amplitude of the ML direction graph, 103.15 mm, is significantly smaller than that of the AP direction, 464.57 mm. This observation aligns with the anticipated findings, given that the stance of the subject is wider in the AP direction when the subject is standing on the left side of the plate. Furthermore, it is evident based on analyzing the time series graphs that they correspond to the COP position for a left-side stance. This is indicated by the AP displacement crossing the zero axis, as the computed coordinates for COP span both sides of the force plate. In contrast, the time series graph of ML displacement remains below zero, which is accurately representative of the subject not moving to the right side of the force plate, thus remaining on the negative x axis.

The results provide a visual confirmation of the system's ability to accurately track and represent the Center of Pressure (COP) based on the subject's position on the force plate. This is particularly evident in the stabilograms, which directly correlate the COP position with the subject's stance on each side of the force plate. The stabilograms confirm the validity of the data being collected and the accuracy of the measurements while the time series graphs showing displacement in both the Medio-Lateral (ML) and Anterior-Posterior (AP) directions offer a clear and concise visual representation of the subject's movement over time. The figures not only validate the testing approach but also allow for an easy comparison of displacement in the two directions. Moreover, the figures enable a more intuitive understanding of the data. The plots transform complex numerical data into a format that is easier to interpret, thereby facilitating a more comprehensive analysis. The visual nature of the graphs allows for immediate recognition of patterns, trends, and anomalies, which might be less apparent in a purely numerical format.

In order to examine positional COP reproducibility from the force plate, a method similar to Huang et al. [51] was used. A dumbbell was placed at eight different locations as shown in Table 4. Each location was tested 10 times. Data was collected for both a flat BASE condition, as well as a 5 degree tilted condition (shown in Table 5). The percentage of error for each point was calculated.

Tested Points		Average Measurements of Tested Points		Percentage of Error	
X [mm]	Y [mm]	X [mm]	Y [mm]	X %	Y %
0	0	0	0	0	0
0	7	0	7	0	0
0	4	0	4	0	0
0	-7	0	-7	0	0
0	-4	0	-4.1	0	2.5
4	0	4	0	0	0
7	0	7	0	0	0
-7	0	-7.1	0	1.43	0
4	0	4	0	0	0

Table 4: Mean and standard deviation values of eight locations on the force plate at flat condition.

Tested Points		Average Measurements of Tested Points		Percentage of Error	
X [mm]	Y [mm]	X [mm]	Y [mm]	X %	Y %
0	0	0	0	0	0
0	7	0	7.2	0	2.86
0	4	0	4	0	0
0	-7	0	-7.2	0	2.86
0	-4	0	-4	0	0
4	0	4.1	0	2.5	0
7	0	7	0	0	0
-7	0	-7.3	0	4.29	0
4	0	4	0	0	0

Table 5: Mean and standard deviation values of eight locations on the force plate at the angled condition.

The maximum percentage of error in the no tilt condition for the X coordinates was 1.43%. The maximum percentage of error in the no tilt condition for the Y coordinates was 2.5%. The percentage of error in the tilt condition for the X coordinates was 4.29%. The maximum percentage of error in the tilt condition for the Y coordinates was 2.86%

Biomechanics show that an increased load on one limb is mirrored by an equal and opposite unload on the opposite limb [35]. Vertical reaction forces under each foot, left and right, alternate completely out of phase with each other, and typically fluctuate about the 50% bodyweight threshold. An example of this is when right hip abductors could become more active and increase right limb loading from 40 to 45%, which would result in an instantaneous unloading of the left limb from 60 to 55%. In order to show that the force plate is capable of collecting data to output this pattern, MATLAB code was written (Appendix C) to calculate the fluctuations in movement. The code takes an input of a subject's previously measured weight in kilograms. The code then reads a Microsoft Excel file containing information about left side force readings and right side force readings, and calculates the body weight percentage. Figure 14 shows an example of output results from the code for a subject standing on the force plate viewing a rolling visual with parameters of 60 degree/second clockwise rotation during a quiet stance on a zero degree tilt.
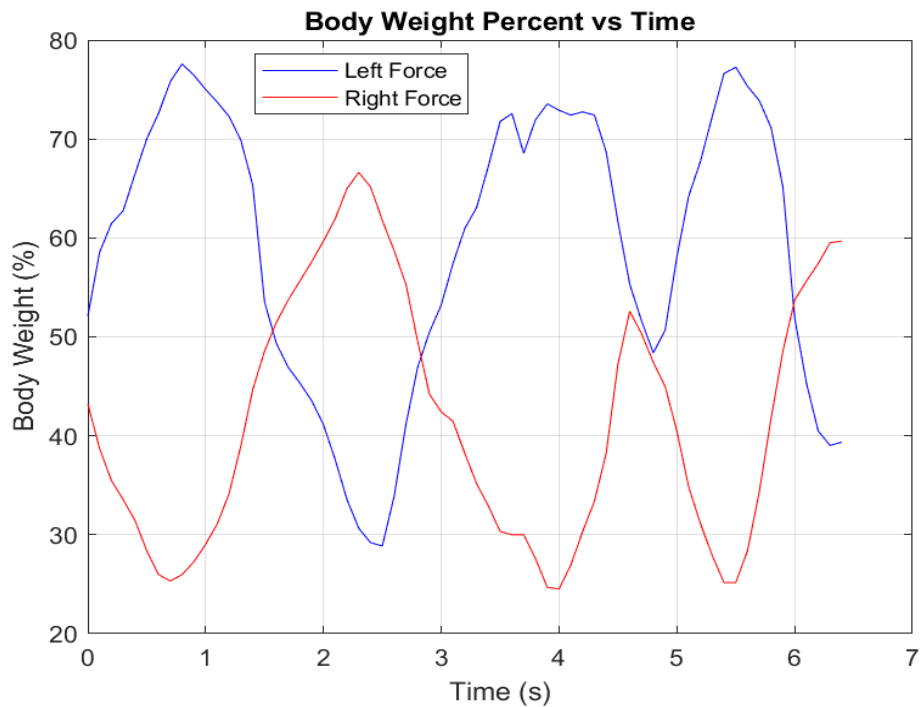
Figure 14: Plot of limb loading relationship over time.

In Figure 14, the horizontal axis shows the time in seconds starting from zero. The Y axis shows body weight percentage. The blue line represents forces obtained from loading of the left limb and the red line represents forces obtained from loading of the right limb. The results are relatively consistent with Winter's study [35], as they are out of phase and fluctuate about 50% body weight. It is important to note, however, that although they fluctuate about that point they do not do so perfectly. The variance can be attributed to the load cell readings themselves, as with this particular system, they can get "sticky" and cause slight overshoots or undershoots in their force output readings during use (+/-2% full scale error). The variability likely is the reason the graph does not fluctuate exactly about 50% because the biomechanical assumption made to create the graph is that the total weight remains constant for each sample of data taken. However, for the purposes of being able to distinguish between the loading and unloading relationships, this variability is acceptable as it remains under 5%.

5.4 Xsens Motion Capture

Xsens MVN Awinda (Enschede, Netherlands) is a system designed for Inertial Measurement Unit (IMU) motion capture. The system is comprised of 17 wireless IMU sensors, each equipped with a gyroscope, accelerometer, and magnetometer. Additionally, the system includes an Access Point (AP), velcro strips, connection wires, chargers, a software dongle license, and a backpack to store the components. The Xsens Analyze software can be downloaded from the Xsens website to be used for data capturing, and the AP facilitates data communication between the sensors and the computer. Prior to initiating a capture of a new data set, anthropometric measurements must be entered into the software. As the software readies for capture, the sensors must be attached to the subject at the manufacturer recommended locations. Once all sensors are in place a calibration process is required. For calibration, the subject is required to stand in an N-pose, standing upright with their arms resting on the sides of their thighs. The subject must remain in the pose for a few seconds, then walk a few steps forward in a straight line, turn around, walk back to the starting position, and turn to face in the direction of the original starting position. Following the calibration, the subject must remain stationary for approximately 30 seconds to allow for filters to fully connect. If deemed necessary, the subject can orient themselves towards the desired global x-axis direction prior to applying the calibration on the

software. Once the calibration is completed, data capture can commence. Xsens Analyze software saves the capture files in .mvn format, which can only be opened using Xsens software. However, for the convenience of processing data further without access to the Xsens software, Xsens offers the option to export data files in .3cd, .bvh, .fbx or .mvnx formats.

Figure 15: The Xsens MVN Awinda IMU system (Movella, Henderson NV) consisting of 17 wireless IMU sensors attached via velcro strips.

Specification	Xsens Awinda	Vicon Marker Based MoCap
Technology	Inertial Measurement Units	Optical markers
Tracking method	IMU based- accelerometers and gyroscopes	Camera-based, detects retroreflective markers
Accuracy	Sub-millimeter to millimeter level accuracy	Sub-millimeter accuracy
Setup	Wireless sensors attached to body	Multiple cameras placed around capture volume
Portability	Highly portable/wireless nature	Not portable, requires cameras in fixed setup
Ease of Deployment	Quick setup and calibration	Complicated setup typically requires third party maintenance
Environment	Suitable for use indoors and outdoors	Indoor, controlled environment usage
Advantages	Portable, easy to set up and deploy. Suitable for dynamic movements	High spatial accuracy. Reliable tracking in controlled conditions
Disadvantages	Lower accuracy in comparison to optical systems. Limited relative positioning without external reference.	Less suitable for dynamic environments. Requires line of sight. Careful calibration. High cost and setup complexity.
Cost	$10,000+	$50-200k+

Table 6: Comparison of specifications of the Xsens Awinda vs Vicon MoCap.

For the purpose of this thesis, the Xsens Awinda motion capture system was chosen in part due to its comprehensive data output, which is conducive to the analysis of various aspects of human biomechanics. The advantages of the Xsens Awinda system over traditionally used marker-based motion capture systems include its portability and cost effectiveness. However, a challenge associated with the integration of the Xsens Awinda into this gamification system is the extensive volume of raw data generated. Consequently, a significant portion of research time was dedicated to identifying relevant parameters for analysis, particularly in relation to the impact of visual roll. The primary focuses of analyses done using this system will be on COM and segment positioning, as these elements can be particularly effective for conducting further research into balance. To validate the applicability of the Xsens Awinda system for use in the gamification training system, it was essential to confirm its ability to detect changes in shifts in a person's COM both in the ML and AP directions in response to alterations in visual cues.

For validation, the COM of a subject was monitored under two distinct conditions, in which a transition between two states occurred at the midpoint of the experiment's duration. To start, the subject was asked to keep their eyes open while maintaining upright posture and looking at a fixed point on a wall 2 meters away. The subject's feet were placed with their heels being approximately 10 cm apart. The subject was instructed to close their eyes and maintain their posture as well as they could after hearing a verbal cue, which occurred at approximately 30 seconds after the start of the test. The total length of the trial was 1 minute long. The Xsens Awinda sample rate was 60 Hz.

The Xsens was capable of discerning the shift in conditions, as evidenced by a change in the amplitude range of the COM data. Prior to the midpoint, the amplitude range was smaller, which was indicative of the subject's stable stance with their eyes open ("Eyes Opened Condition"). Following the transition to the "Eyes Closed Condition", the amplitude range exhibited an increase, thereby reflecting a greater variability in the COM position until the end of the trial. The pattern was observed in both the ML and AP directions. Having the ability to distinguish a change in amplitude range can provide insights into a subject's balance control by revealing whether they have a greater degree of fluctuation in either the AP or ML direction [52]. The graphical representations of the COM data for both the ML and AP directions, as seen in Figure

16 and 17 below, for both the ML and AP directions, corroborate these observations. Both graphs demonstrate a noticeable alteration in the data trends that begin approximately at the halfway point of the experiment, corresponding to the change of the visual condition, thereby confirming the sensitivity of the Xsens system to changes in the subject's visual sensory conditions.

A MATLAB code was created in order to calculate several statistical measures pertaining to the COM data provided by the Xsens system. The code is capable of analyzing the standard deviation, variance, range, and mean absolute deviation of data taken over time (using equations 3-6). The resulting graphs are shown in Figure 18. For the trial conducted, the standard deviation for the "Eyes Opened" condition was 0.0001442 mm, and for the "Eyes Closed" condition was 0.00027088 mm. The deviations indicate a greater dispersion in the COM x-direction when the eyes are closed, suggesting an increase in postural sway. The variance values are 2.0793e-08 and 7.3376e-08 in the "Eyes Opened" and "Eyes Closed" conditions, respectively. The higher variance in the "Eyes Closed" condition further corroborates an increased dispersion observed in the COM data. The range values for the "Eyes Opened" and "Eyes Closed" conditions are 0.00073628 and 0.0015689, respectively. The larger range in the "Eyes Closed" condition suggests a wider spatial distribution of the COM in the x-direction. The Mean Absolute Deviation (MAD) values for the "Eyes Opened" and "Eyes Closed" conditions are 0.0001158 and 0.00021761, respectively. The higher MAD in the "Eyes Closed" condition suggests a greater average deviation from the mean position.
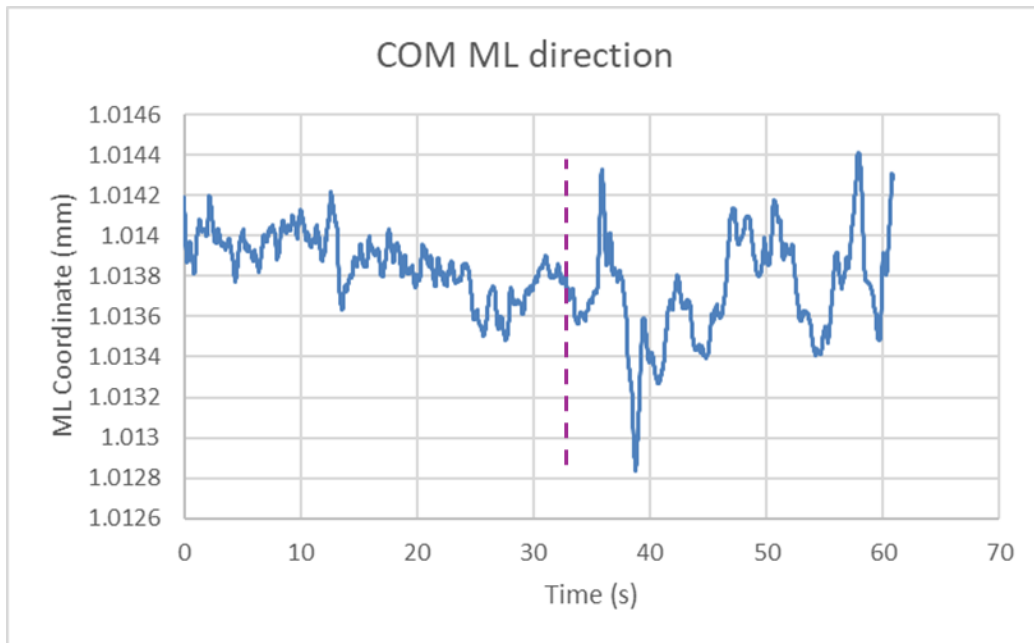
Figure 16: COP in the ML direction (mm) over time for the Eyes Opened vs Eyes Closed conditions. The dashed line denotes where changes begin to become visible after visual condition changed.
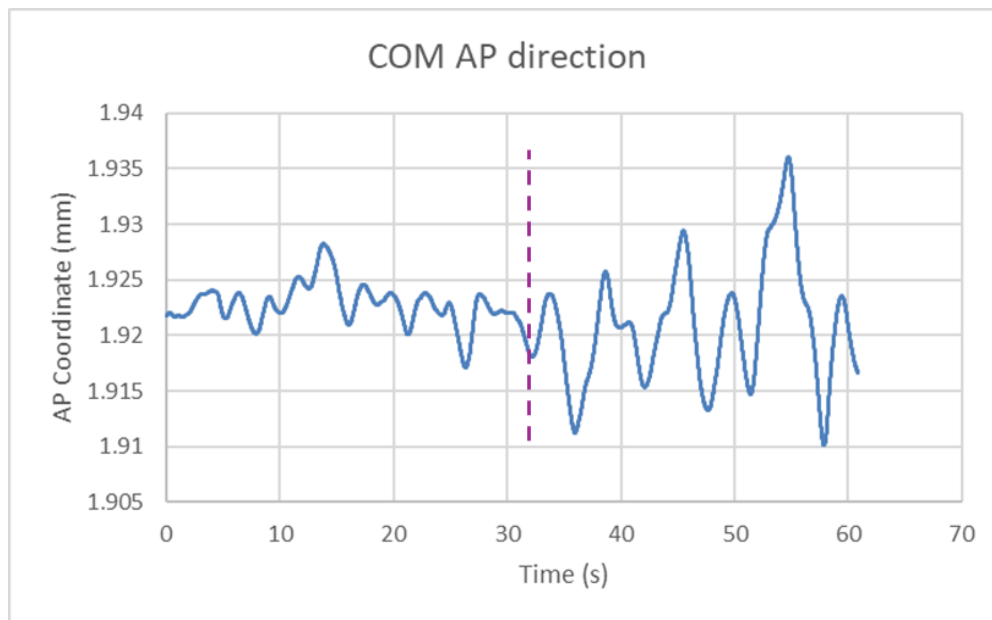
Figure 17: COP in the AP direction (mm) over time for the Eyes Opened vs Eyes Closed conditions. The dashed line denotes where changes begin to become visible after visual condition changed.

41

In Figures 16 and 17, it is evident that there is a change in range of data by looking at the time series beginning at approximately the 32 second mark where the visual condition changed. There is a larger difference between the min and max excursions before the 30 second mark where the visual condition changed. As shown in Figure 16, for the ML direction, the maximum excursion for peak to peak value during the Eyes Opened condition was 0.00074 mm. For the Eyes Closed condition, the maximum excursion for the peak to peak value was 0.00157 mm. As shown in Figure 17, for the AP direction the maximum excursion for peak to peak value during the Eyes Opened condition was 0.0099 mm. For the Eyes Closed condition, maximum excursion for the peak to peak eyes value was 0.0257mm. These observations show that the largest sway occurred in both the AP and ML direction during the eyes closed condition. This thereby supports the theory that removing visual stimulus causes larger excursions during sway.

$$\text{Mean: } \mu = \frac{1}{n}\sum_{i=1}^{n} x_i \tag{3}$$

$$\text{Standard Deviation: } \sigma = \sqrt{\frac{1}{n-1}\sum_{i=1}^{n}(x_i - \mu)^2} \tag{4}$$

$$\text{Variance: } \sigma^2 = \frac{1}{n-1}\sum_{i=1}^{n}(x_i - \mu)^2 \tag{5}$$

$$\text{Mean Absolute Deviation: } MAD = \frac{1}{N}\sum_{i=1}^{n} x_i - \mu \tag{6}$$
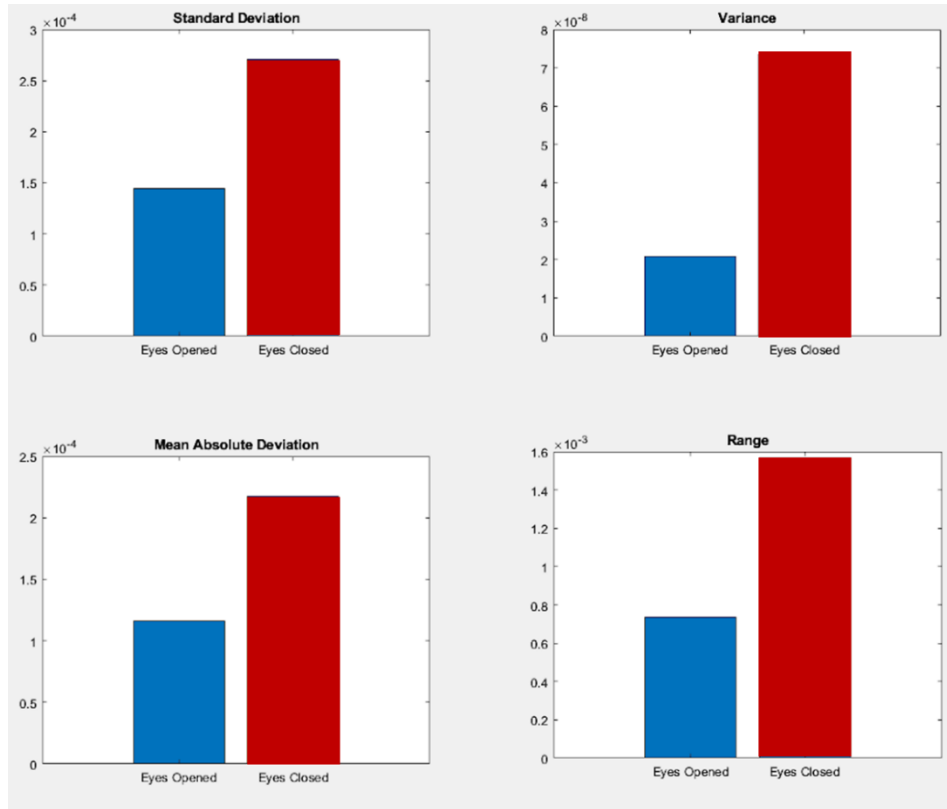
Figure 18: Bar graphs representing differences in values of standard deviation, variance, mean absolute deviation, and range for the Xsens COM and ML data.

5.5 Virtual Reality

To maintain upright posture, gait, and most motor activities, one must have the ability to perceive spatial orientation in relation to gravity. In healthy individuals, substantial interactions between roll motion and spatial orientation have been observed. Studies conducted by Whitney et al. and Nishida et al. [36, 37] suggest regions of the cortex sensitive to motion interact with regions that are involved in determining the gravitational visual vertical (such as the parieto-insulo-vestibular cortex [38]) and those imperative for visuospatial localization of static stimuli in 2-D space (such as the parieto-occipital cortex).

While visual roll has been the subject of numerous studies, the incorporation of VR technology in this field has been limited, primarily due to the novelty of headset based VR. The development of this technology has opened up new avenues for allowing the manipulation of virtual scenes to offer more immersive visual experiences compared to traditional screen projections. The integration of VR into this gamification system brings significant benefits which can potentially be used for rehabilitation or training purposes. It allows individuals to easily adopt a variety of body positions -including sitting, squatting, leaning, or dynamic poses- without impact on their visual perspective. The use of VR eliminates the need for a subject to be in a specific viewing direction, or having to alter their head position to view a screen, as in the study conducted by Tanahashi et al [41], where the range of motion was restricted and could have been subconsciously influenced by spatial awareness.

The HTC Vive Pro 2 (Taipei, Taiwan) is a state of the art virtual reality system designed for immersive gaming, offering a high degree of immersion and realism. The system includes the Vive Pro 2 headset, equipped with dual 2.5K AMOLED displays, each offering a resolution of 2448X2448 pixels, providing a wide 120-degree field of view. In addition to the headset, the package comes with a link box, a DisplayPort cable, a USB 3.0 cable, power adapter, and a cleaning cloth. The Vive Console software can be downloaded from the HTC website and is used for setting up and managing the VR experience. Prior to initiating a VR experience session, a user's physical dimensions and play area need to be configured within the software. The headset and controllers must be connected to a PC and positioned as recommended by HTC. A

calibration process is necessary to ensure optimal tracking and performance. A user must stand at the center of the play area, with the headset and controllers visible to the base stations.

The HTC Vive Pro 2 employs SteamVR tracking, a high precision tracking system that provides 360-degree coverage of movements. The tracking system relies on two external sensors and two motion controllers, each equipped with 24 built in sensors. The tracking system works by emitting light from the base stations. The consistent movement and frequency of each laser's movement allow time to be used as a reliable measurement of the angle and distance from the base station to the tracked object. Because of this, latency of the viewing field is minimal. This is achieved through a combination of high refresh rates and low latency tracking. The refresh rate is 120HZ, ensuring that the virtual environment responds quickly and smoothly to head movements.

Feature	HTC Vive Pro 2	Oculus Quest 2
Manufacturer	HTC	Meta
Device type	PC-powered VR	Standalone VR
Optics	Dual element Fresnel lenses	Fresnel Lenses
IPD range	57-70mm (hardware adjustable)	58-68mm (hardware adjustable)
Display Type	2 LCD binocular	Single fast switch LCD binocular
Resolution	2448 x 2448 pixels	1832 x 1920 pixels
Refresh rate	120 Hz	120 Hz
Field of view	116 deg horizontal, 69 deg vertical	97 deg horizontal, 93 deg vertical
Retail Price	$1399	$350

Table 7: Specifications between two available VR systems, the HTC Vive Pro 2 and Oculus Quest 2.

The HTC Vive Pro 2 was chosen for the purposes of this thesis as it has a higher resolution rate of 2448 x 2448 pixels than the Oculus Quest 2's 1832 x 1920 pixels, which can provide sharper and more detailed visuals. Also, the HTC Vive Pro 2 has a field of view of 116 deg horizontal, 69 deg vertical, which is wider than Oculus Quest 2's 97 deg horizontal, 93 deg vertical, because a wider view provides for a more immersive VR experience as it covers more of a user's natural visual field.

5.6 Visual Conditions

The random dot pattern, originally adapted from Brandt et al., is a common tool used in visual perception research studies. The random dot pattern consists of randomly distributed dots which move coherently. Using a random dot pattern provides a way to represent visual motion without explicit environmental context, allowing researchers to isolate effects of motion perception without the influence of specific objects or scenes. Experimental control offered in this manner allows for researchers to precisely control motion parameters including speed and direction, in order to investigate how they influence vection, thereby providing insights into the mechanisms of visual perception. The human brain interprets motion based on visual cues such as optic flow [39]. When viewing random dots moving in a circular manner, the brain perceives evidence of self-motion due to the dots' movement simulating the expected pattern of motion that occurs when rotating around the roll axis. Because of this, researchers have consistently employed the use of this stimulus in brain studies related to circular vection.

The visual developed and displayed for the purposes of visual roll effects in this thesis is a random dot pattern of white dots on a black background. In order to collect data samples on perceived subject verticality, a line that can be manipulated by the user using game controllers can also be included in the visual field, which can be seen in Figure 19: The speed of rotation of the random dot pattern visual can be manipulated easily in the Unity Software, and is measured in degrees per second. The direction of rotation of the pattern can also be changed.
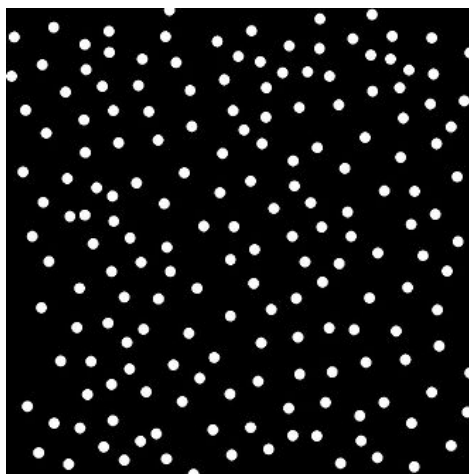
Figure 19: Random dot pattern used in VR rolling visual.

A Subjective Visual Vertical (SVV) assessment is a clinical test that gauges a person's ability to discern whether an object is in a vertical position, without the use of real vertical reference. The procedure involves asking a subject to align a bar with a position that the individual judges to be vertical. The amount of tilt of the individual's response position, relative to the true Earth vertical, is quantified in degrees [42]. The quality of the visual being presented [43,44] and vestibular otolithic information [45] both affect an individual's ability to determine whether the bar is aligned with the true vertical. This information is instrumental in encoding the static gravitational orientation and cephalic linear acceleration movements, which can in turn contribute to the maintenance of posture and balance. In order to collect data samples on perceived subject verticality, a line that can be manipulated by the user using game controllers can also be included in the visual field.
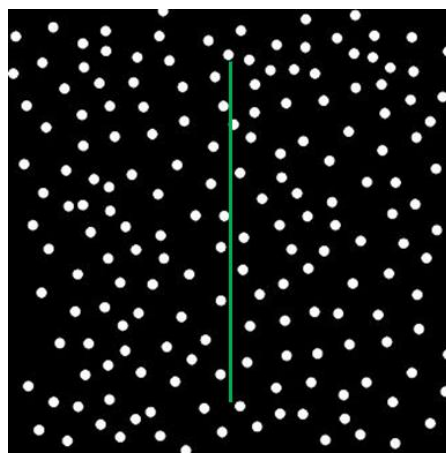
Figure 20: SVV testing visual of random dot pattern and movable line.

Figure 21 is a bar graph that visually encapsulates the results of 15 trials from an example of the SVV test. Each bar represents a single trial. In each trial, a line located in the center of the viewing field is initially set at a random, non-vertical angle. The subject's task is to manipulate this line using the VR hand controllers, aiming to align it to their perception of the vertical position. The bar graph is an output integrated into the created game. The results provide a visual summary of the subject's performance results across all trials conducted. From the averaged results, the deviation of a subject's perceived vertical from the true vertical can be quantified. The left side of the graph indicates the degree to which the subject's perception was tilted to the left of the true vertical. The right side of the graph shows the degree of tilt to which the subject's perception was tilted to the right of the true vertical. By convention, positive and negative values indicate that the SVV line is tilted clockwise (CW) and counterclockwise (CCW), respectively. In between each trial, the line is reset to another random angle by the test administrator.
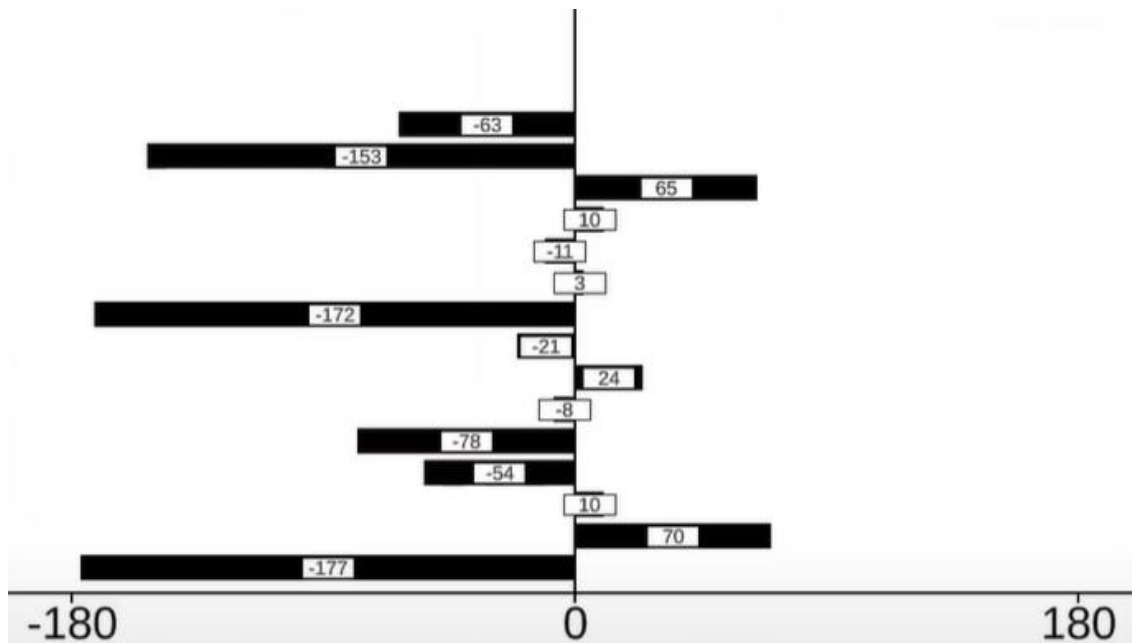
Figure 21: Visual representation of a subject's visual vertical results.

A greater amount of bars displayed on the right of the graph provide an indication that a person perceives the world as being more tilted to the right than it actually is. Conversely, more bars to the left of the graph provide an indication that a person perceives the world to be more tilted toward the left. Figure 21 suggests that the individual has a stronger bias toward viewing the world tilted to the left.

In between each vertical alignment trial of the test, the subject was instructed to use the controllers to set the line to their perceived SVV. They were verbally instructed that the right controller trigger can be clicked to rotate the line in a clockwise motion, and that the left controller trigger can be clicked to rotate the line in a counterclockwise motion. The subject was then given verbal instruction that once the subject believes that they have aligned the computer generated rod to be vertical, they will give a verbal cue to the administrator saying "OK". After the administrator heard the verbal cue, they then manually reset the line to another random position. This process was repeated 15 times for each of the trials. Once the 15 were complete, the rolling visual was stopped, and the subject was asked to remove the VR headset. The subject was then instructed to step off of the platform whilst it was moved into position for the next trial.

5.7 Body Segment Analysis
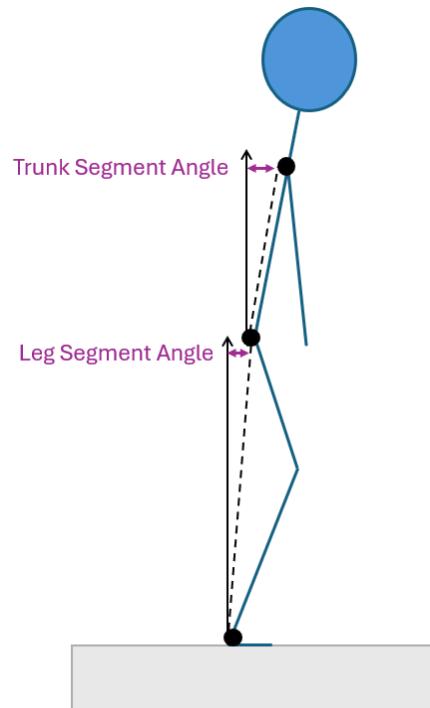
Figure 22: Schematic of a sagittal view of subject in quiet stance on the force platform. Displacements of the trunk and leg segments were defined based on the angular displacements from the vertical. Black circles designate placement of sensors being analyzed for two segment modeling.

Kinematic data was simultaneously recorded using the Xsens Awinda system, at a 60 Hz sampling rate. Markers were placed as suggested by the Xsens Awinda manual, however for the purposes of the two segment analysis, data from the shoulders, pelvis, and foot sensors were analyzed. The trunk segment was defined as the distance between the shoulders and the head of the pelvis. The leg segment was defined as the distance between the head of the pelvis and the ankles. Data provided from the Xsens allowed for analyses to be performed in both the ML and AP planes, and the respective coordinate directions were used in order to complete their respective analyses.

Postural analysis is a multifaceted challenge which is attributed largely due to numerous segments of the human body that come into play during quiet stance, as well as more dynamic movement, as indicated in various studies. For the purposes of this thesis, the trunk and leg

segments were analyzed. The decision was influenced by research that explored the manner in which these segments respond to changes in sensory information. This is important as the gamification system can be used to alter sensory information in multiple ways, including dynamic movement of the support surface, as well as changes in visual input from the VR.

The angular displacement of the trunk segment was defined as the angle created by the point between the shoulder, the head of the pelvis, and the vertical, as shown in Figure 22. The angular displacement of the leg segment was defined as the angle formed by the point between the head of the pelvis, the point between the ankles, and the vertical. Positive angles indicate movement in the positive axis directions. For the ML direction, the angular displacements were measured in the ML plane. For the AP direction, the angular displacements were measured in the AP plane.

MATLAB code (Appendix D) was written to compute and plot cross correlation functions to examine how strongly correlated signals from the force plate and the Xsens Awinda systems were, since the gamification system itself consists of separate subsystems. If a cross correlation function graph looks like a perfect triangle with a peak lag at zero and correlation of 1, it suggests that the two signals being compared are extremely similar or even identical. Figure 24 below shows the cross correlation function comparing COM ML data from the Xsens Awinda to the COM ML data gathered from the force plate of the gamification system. Figure 23 shows the cross correlation function comparing the COM ML data from the Xsens Awinda to the L3 (spinal position) ML data from the Xsens Awinda. The L3 spinal position was chosen since, according to biomechanics, the L3 position of the spine and the body's center of mass positions should be extremely highly correlated to each other. The data gathered was from a subject performing a quiet stance, flat surface trial. Figure 24 shows a peak correlation of 0.71 at a lag value of 68. The high correlation value indicates a strong correlation between the two signals, suggesting a similarity between the two sets of data. The lag, since it is not 0, indicates that there is a slight time delay between the two systems. However, for the purpose of using this gamification system, the lag is small enough to be considered to be negligible, as the time scale of the trials being examined is large. Figure 23 shows a peak correlation of 1 and a lag value of 0. This confirms that data taken within the Xsens system at different sensors relative to each

other do not experience a lag and are extremely highly correlated. This result was expected, as the Xsens Awinda IMU's are all calibrated and a part of the same system.
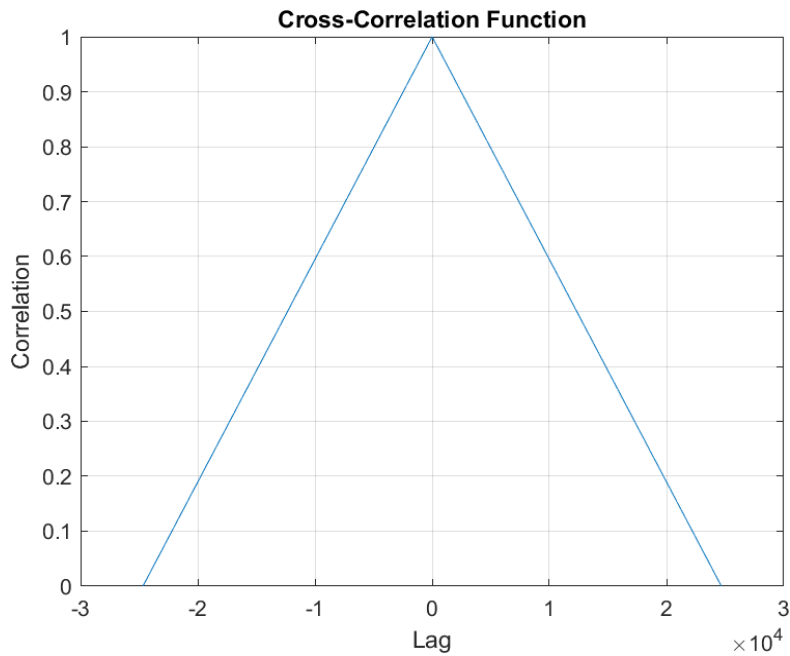
Figure 23: Graph of the cross correlation function comparing the COM ML data from the Xsens Awinda to the L3 (spinal position) ML data from the Xsens Awinda.
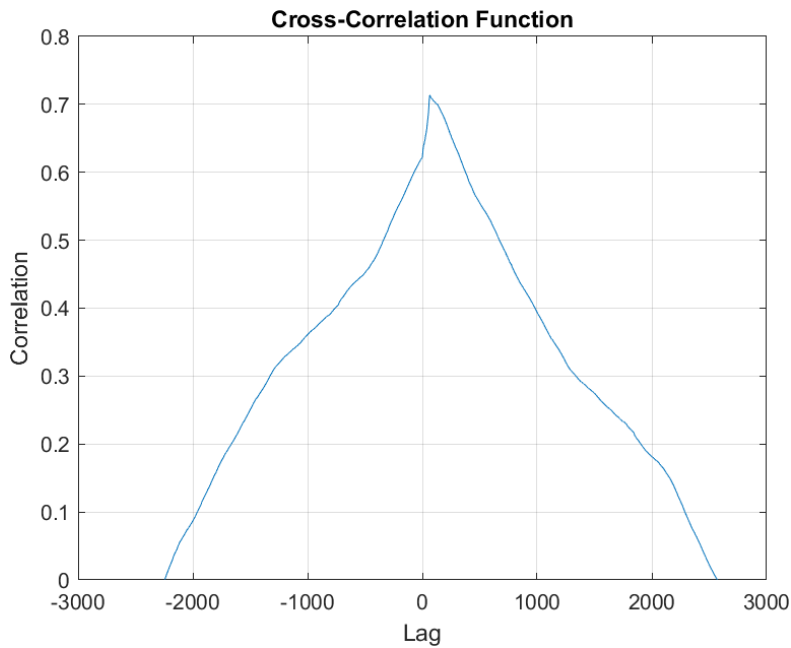
Figure 24: Cross correlation function comparing COM ML data from the Xsens Awinda to the COM ML data gathered from the force plate.

6.0 SUBJECT TESTING

The system was used to perform testing on a subject in order to further investigate the ability of the system to gather valuable balance information. Testing procedures were separated into several parts with three different conditions. The conditions were eyes opened, eyes closed, and VR rolling visual presence. The testing was conducted in a lab where the BASE gamification system was located.

Subject:

Every test performed for this study was done by one subject.

Testing Conditions:

Testing conditions are meant to be in a pose that is relaxed and natural, without restriction to the human body. Every test performed for this study was done by one subject. Exclusion criteria for study participation is a history of a concussion or any other neurological disorder impacting balance, and uncorrected vision. The subject gave informed consent prior to starting the study. The subject was asked to stand with their arms hanging comfortably at their sides. The position of the feet was standardized at an angle of approximately 20 degrees between each foot from the vertical marking on the platform, with their feet in a comfortable, hip width apart to emulate their natural standing position.

In order to not introduce bias, the subject was not told what the purpose of the experiment is. They were only told that they would be standing on a mechanical platform that could be moved into different angled positions, and would be required to have a VR headset on and play a game. In between different platform angle trials, they would be asked to step off of the platform so that it can be set to its new position. The subject was instructed to not look down when getting back on the BASE platform in order to eliminate potential visual bias. The test administrator positioned their feet for them and assisted them with getting on and off of the BASE platform safely.

Before stepping onto the BASE platform and beginning any testing, the subject was first asked to perform a Romberg test on flat ground to confirm that they can maintain normal, unassisted balance. The Romberg test was first described by Moritz Heinrich von Romberg, who found that patients with neurosyphilis often complained of increased unsteadiness in the dark. It was found that symptoms could also be elicited in several different conditions that affect proprioception. The Romberg test is described as a method of subjective testing for vestibular dysfunction.

The subject was asked to remove their shoes and stand with both feet together. They were then asked to cross their arms in front of their body. For the first part of the test, the subject was asked to keep their eyes open and try to stand still for 30 seconds. It is important to note that the administrator was facing the patient with their arms out, without touching them, to catch the patient if they fell. For the next part of the test, the subject was asked to close their eyes and try to stand still for 30 seconds while the administrator watched. In order to proceed with using the BASE system, the results of the performed Romberg test should be normal. Abnormal results noticed by the test administrator should be reported immediately to a clinician and the subject should not proceed with the experiment.

Romberg Test Result Options	
Negative Result (Normal)	• Minimal Swaying Occurs • Patient is able to complete both legs of the test
Positive Result (Abnormal)	• Failure to keep the eyes closed, a loss of balance that requires the feet to move • Increased body sway • Patient falls

Table 8: Romberg Test Result Options.

Before the subject stepped onto the platform, they put on the harness. The administrator then clipped the harness to the BASE support. The subject then stepped onto the platform and was positioned onto the force plate with the appropriate standardized foot position as instructed. Prior to putting on the head mounted display, the subject was asked to stand as normally upright as possible for 20 seconds, and only to take a step to prevent falling. The subject then put on the head mounted VR display. The administrator of the test then gave the subject each of their hand controllers. The subject was given verbal instructions to stand upright and maintain their posture throughout the entire test for each trial.

7.0 RESULTS

7.1 Test Conditions

An SVV test was then conducted on the subject while wearing the VR system and standing on the BASE platform. The test was conducted under four distinct platform conditions. In between each movement of the BASE platform to its new position to begin a new trial, the subject was instructed to step off of the platform, and was allowed to take a one to two minute break. Each platform tilt direction was conducted at an angle of 5 degrees.

Platform Tilt Direction	Visual Roll Condition	Avg Deviation from Vertical on Right (deg)	Avg Deviation from Vertical on Left (deg)	Tilt Bias
Forward	60 deg/sec CW	2	1.5	Right
Forward	60 deg/sec CCW	2.3	1.7	Right
Right	60 deg/sec CW	1.8	1.6	Right
Right	60 deg/sec CCW	1.1	1.8	Right
Back	60 deg/sec CW	1.9	2.9	Left
Back	60 deg/sec CCW	1.4	4.4	Left
Left	60 deg/sec CW	1.7	1.4	Right
Left	60 deg/sec CCW	1.1	2.6	Right

Table 9: SVV test conditions and results of subject responses.

In Table 9, the "Avg Deviation from the Vertical" is an average amount of degrees that the subject's submitted responses deviated from the true vertical, taken across the 15 trials for each tilt condition. For average deviation on the right, the average was taken of all trial responses that were reported as to the right of the true vertical (indicated as positive degree values, as shown above in Figure 21 graphical representation). For average deviation on the left, the average was taken of all trial responses that were reported as biased to the left of the true vertical (indicated as negative). The duration of each test took approximately 4 minutes for the subject to complete all of the trials. If 8 or more responses per test were recorded as biased towards the right, the subject was categorized as having their perception of the vertical to be biased toward the right. If 8 or more responses per test were recorded as towards the left, the subject was categorized as being biased towards the left. The results of these tests show that the subject perceived the vertical to be generally towards the right of the true vertical in all platform tilt directions except for the backward tilt direction, where there were more responses of average deviation from the vertical on the left.

7.2 Power Spectrum Density

Power spectrum density analysis was conducted on data gathered to analyze both body segment movement as well as COM movement. In order to do PSD calculations for the leg and trunk segments, data output from the Xsens Awinda system was selected. The trunk and leg segments of the model were created by positions in the X and Y directions of the trunk and leg segments were calculated from raw data output using Excel. A MATLAB code (Appendix E) was used to create vectors to calculate changes in angles over time for the trunk and leg segments. The vectors were then used to perform power spectral density analysis using Welch's method. To calculate and plot PSD analysis results, another MATLAB code was written, as shown in Appendix F.

Figures 25 and 26 show resulting PSD graphs of a subject performing exaggerated sway movements. The exaggerated movements were done to confirm the Xsens measurements were sufficient for PSD analysis. The subject stood with their feet apart at approximately a 10 cm heel

distance on the untilted platform. The subject was instructed to complete repetitive oscillating movements of leaning to the right side as far as they comfortably could without losing their footing, and then returning back to their upright position, for a total of 30 seconds. Data Column 1 in Figures 25 and 26 show the data of the movement over the leg segment in the ML direction. Data Column 2 shows the data of the movement for the trunk segment in the ML direction. The large separation reflects the difference in the dynamics of the segments which is largely dictated by biomechanics.
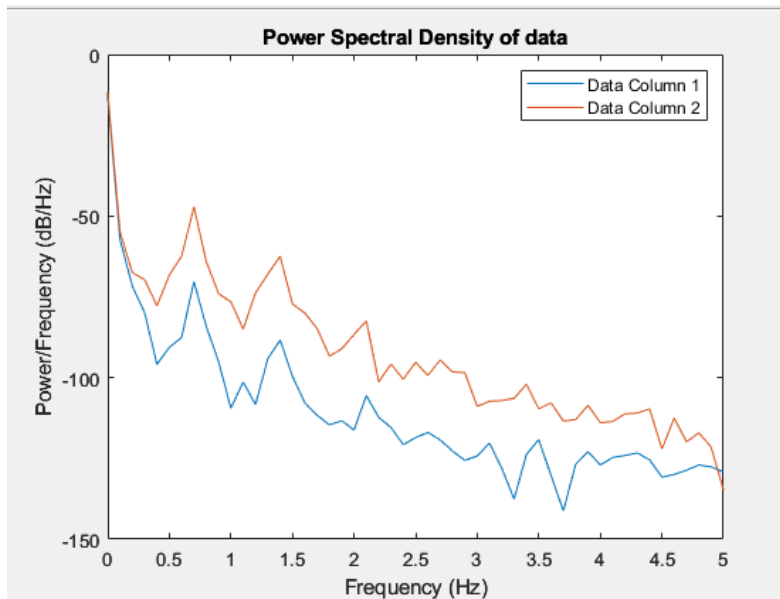
Figure 25: Graph showing data for extreme oscillating movement results where Data Column 1 is the leg segment and Data Column 2 is the trunk segment.
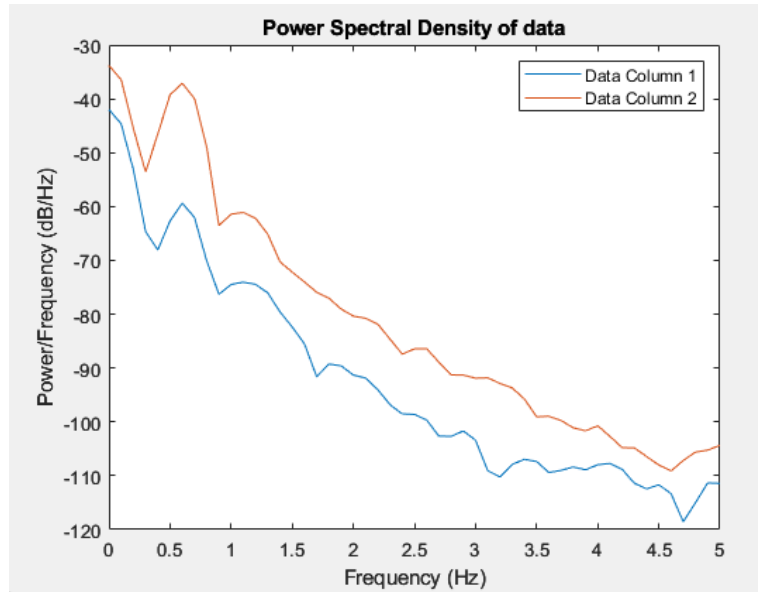
Figure 26: Graph of exaggerated motion in the AP direction where Data Column 1 is the leg segment and Data Column 2 is the trunk segment.

There is a clear separation between the trunk segment data and the leg segment data in both the AP and ML directions with the trunk segment data power being consistently higher than the leg segment data. The separation shows that the Xsens system and corresponding MATLAB code created are capable of distinguishing a difference in the dynamics of the segments.

For testing the sensitivity of the Xsens quiet standing conditions, the experiment was repeated without sway. The subject was asked to stand in a quiet stance on the untilted platform. The total duration of the test was one minute. For the first 30 seconds, the subject was instructed to maintain their upright posture with their eyes open, looking at a fixed point on a wall approximately 10 feet away. For the next 30 seconds they were instructed to close their eyes and continue to maintain their balance. COM data was taken from the Xsens data output for analysis. Figures 27 and 28 show the data plotted for COM in the ML direction. Data Column 1 represents data for the eyes opened condition, and Data Column 2 represents data for the eyes closed condition. Figure 27 shows the data plotted with a window length that was a sixth of the length of the data, while Figure 28 shows data plotted with a window length that was a third of the length of the data. Different window lengths were chosen to assess the impact on the sensitivity of the spectral analysis used to the choice of the window length, as window length can affect the resolution of the frequency analysis.
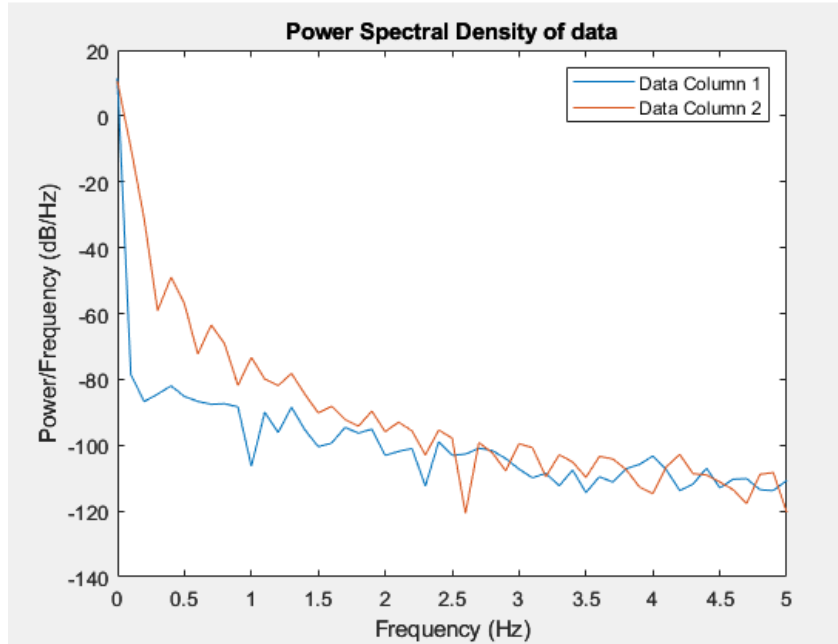
Figure 27: Graph with a window that is a sixth of the length of the data, showing COM motion in the ML direction, where Data Column 1 is the eyes opened condition and Data Column 2 is the eyes closed condition.
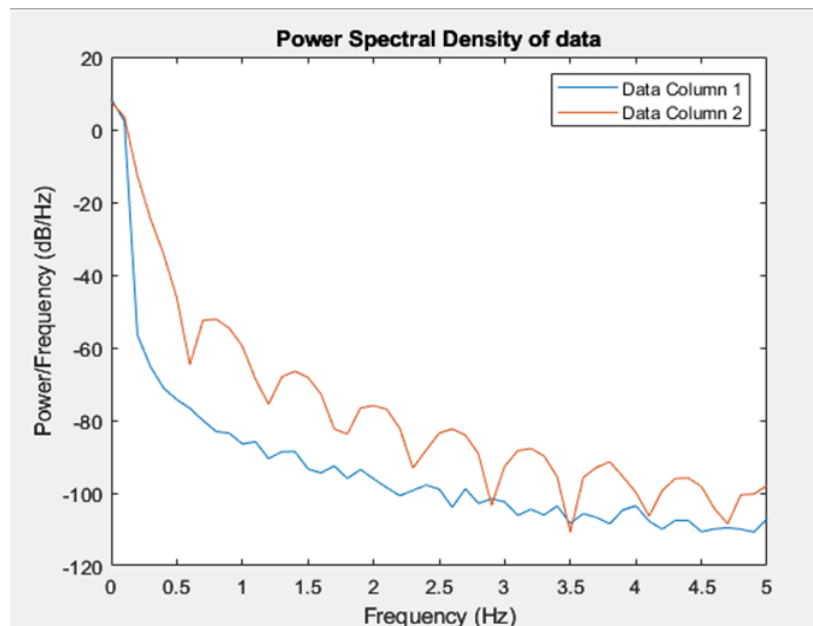
Figure 28: Graph with a window that is a third of the length of the data, showing COM motion in the ML direction, where Data Column 1 is the eyes opened condition and Data Column 2 is the eyes closed condition.

The following test consisted of several trials where the subject was asked to maintain their balance on the BASE under different platform configurations and visual conditions. Table 10 shows the Trial categorizations and their respective conditions. For each tilt direction, the subject was instructed to stand with their feet in the same position on the force plate as stated in the method section above. PSD graphs were then created for each trial.

Trial Number	Tilt Direction	Visual Condition
1	Forward	No Visual Roll
2	Forward	Visual Roll 60 deg/sec right
3	Right	No Visual Roll
4	Right	Visual Roll 60 deg/sec right
5	Back	No Visual Roll
6	Back	Visual Roll 60 deg/sec right
7	Left	No Visual Roll
8	Left	Visual Roll 60 deg/sec right

Table 10: Trial numbers and corresponding platform configurations for Visual Roll vs No Visual roll conditions.
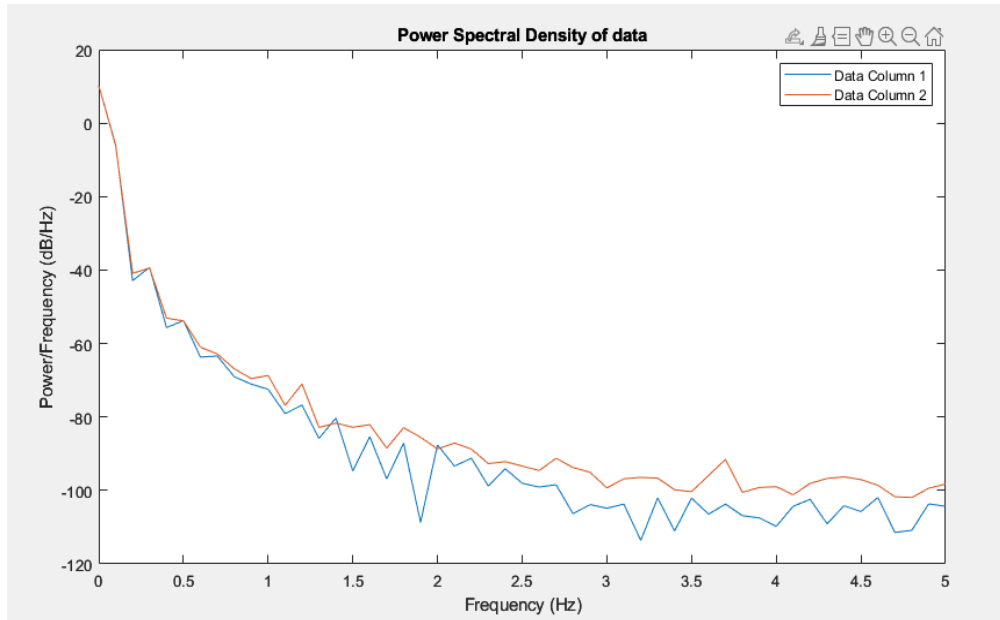
Figure 29: Graph showing Xsens Awinda COM data in the ML direction where Data Column 1 represents Trial 1 and Data Column 2 represents Trial 2.

In Figure 29, Trial 1 and Trial 2 are compared as they had the same platform tilt condition, but different visual conditions ("No Visual Roll" versus "Visual Roll"). The COM is of the subject is analyzed. The movement of the COM of the subject in the ML direction generally exhibits a higher power compared during Trial 2 (Data Column 2) than in Trial 1 (Data Column 1). Although not shown, graphical results were generated for all of the Trials under comparison, each corresponding to a specific tilt direction. The results consistently indicated that the trials conducted under the "Visual Roll" condition demonstrated higher power when compared to those conducted under the "No Visual Roll" condition. The pattern was consistent with all paired sets of data, which included Trials 3 vs 4, Trials 5 vs 6, and Trials 7 vs 8.
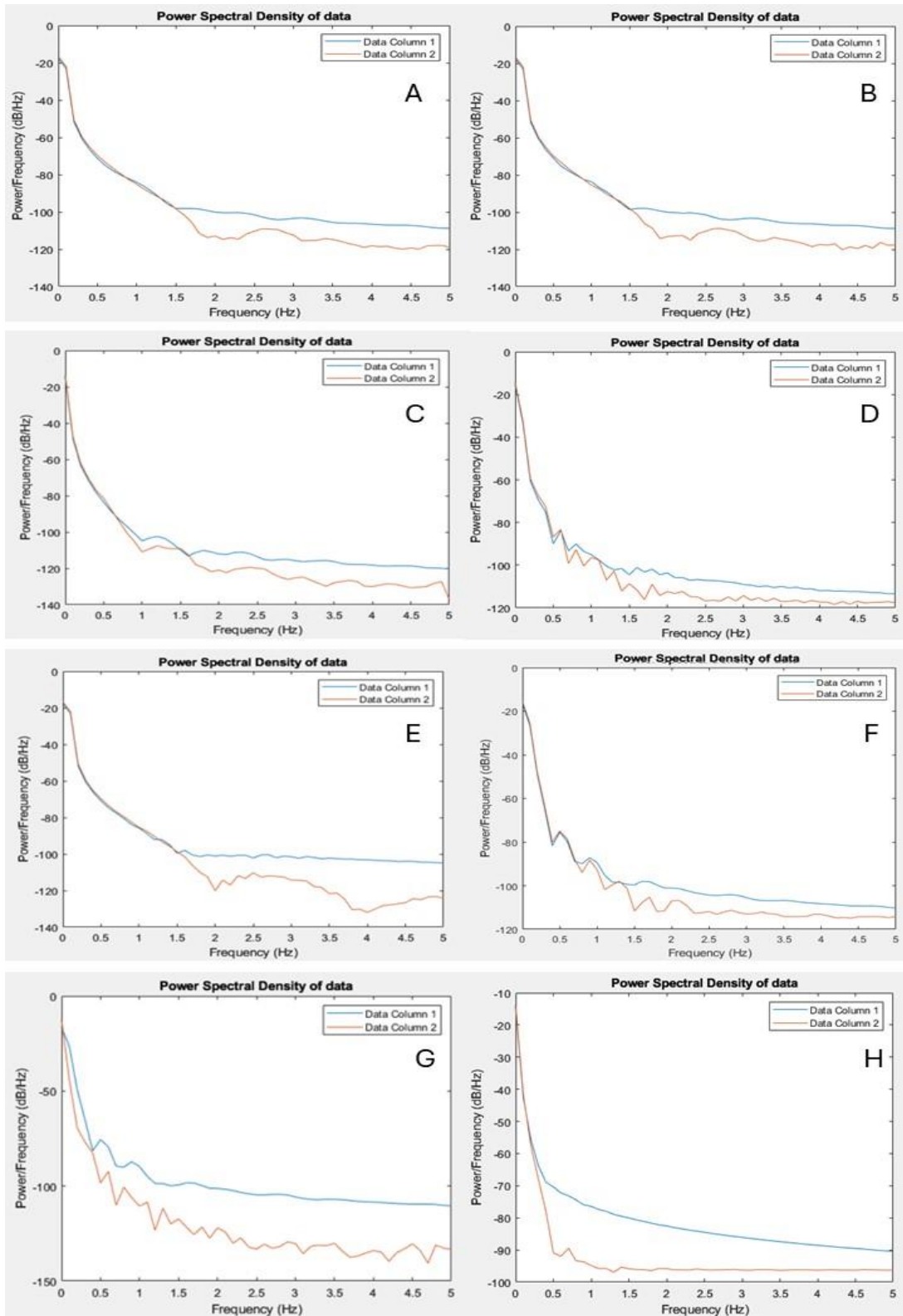
Figure 30: PSD graphs for body segment analysis of each of the 8 trial conditions.

Figure 30 shows PSD graphs of leg and trunk segment data taken for each trial. The data shown is of Xsens Awinda COM data for the ML direction. In the figure, Trial 1 corresponds with graph A, Trial 2 with graph B, Trial 3 with graph C, Trial 4 with graph D, Trial 5 with graph E, Trial 6 with graph F, Trial 7 with graph G, and Trial 8 with graph H. The graphs all show a consistent downward trend for each trial. For graphs D, F, and H, which are visual roll condition trials, the power frequency readings were substantially lower than their "No Visual Roll" trial counterparts (graphs C,E,G). However, graphs A and B, representing the forward tilt condition, showed little to no decrease in power after the addition of visual roll, which was unexpected. The minimal change could be attributed to the subject's biomechanical adaptability. The subject might be more accustomed to forward tilts from their daily experiences, thereby maintaining balance more effectively under this condition. Also notable is that graphs A, B, C, H and F seem to have relatively smoother data than the others, with a reduced amount of spikes overall. Additionally, graph E shows a slight "bounce" shape in the data that increases and then decreases from the 2-4 Hz frequencies.

Some contributing factors in the variation could stem from the application of Welch's method. The window length in particular plays a role into how the data is presented. The combination of the process of segmenting the signal into overlapping sections, applying a window function to each segment, and subsequently averaging the resulting periodograms can introduce a degree of variability into the data. Also, factors of external elements such as subject movement could have also contributed.

8.0 DISCUSSION

Postural control is vital for the maintenance of stability during daily life. Understanding how the human body responds to different conditions, such as platform positioning and visual cues, can provide valuable insights into postural adjustments. An Xsens MVN Awinda IMU motion capture system was used in conjunction with the HTC Vive Pro 2, and a custom made force plate, in order to create a gamification system to quantify and interpret factors critical to balance influenced by postural stability.

The mechanical abilities of the BASE platform allow it to act as a versatile and robust tool for advancing research and applications regarding balance studies. Integrating the BASE platform with VR technology allows for a sophisticated gamification experiences that can be used to go beyond mere visual immersion. The work shown in this thesis supports that the platform can be used to study postural control mechanisms, particularly pertaining to balance, that can be studied in various scenarios. The BASE can be used to accurately simulate both static and dynamic movements. Precise control of the actuators that drive platform motion allows for tilts of up to 20 degrees in all directions. Verification of tilt angles was done using a digital level with high accuracy of +/- 0.2 degrees, further confirming the reliability and reproducibility of the platform's manipulation capabilities.

Initially, the force plate had been designed with springs and a flat metal plate, which gave way to unwanted deflection. The force plate was redesigned using rigid plywood to eliminate deflection issues, which helped to ensure accurate load cell readings and improved user safety of the system. Each of the load cells of the force plate were calibrated individually and verified using known masses. The completed force plate assembly was also verified with known masses at several different locations, demonstrating high repeatability and accuracy in force measurements. Data acquisition from the force plate was streamlined, captured and logged with the use of CoolTerm and Excel. This facilitated detailed analysis of the COP data, which is important for evaluating postural stability. The platform capabilities make way for comprehensive studies to be done on human biomechanics, allowing for assessment of both AP and ML sway patterns.

When trying to analyze data from these two systems, it was important to be able to organize and quantify what should be analyzed. A major challenge of verifying that this system can be used to detect changes in sway was being able to select what data needs to be studied, as well as how to represent the data, as it is all reported in numerical form per frame. The load cells output a large amount of data in numerical form, logging force data at a rate of 10 Hz. The Xsens Awinda outputs a large amount of data, logging at a rate of 60 Hz. For each sensor marker, there is information in the x, y, z directions, there is information on segment orientation in quaternions, in Euler, segment position, segment velocity, segment acceleration, segment angular velocity, segment angular acceleration, joint angles, sensor magnetic field, among others. The subsets that were found to be most useful for the purposes of the studies conducted in this thesis were the segment position and center of mass readings.

The center of pressure is a widely used parameter in the study of biomechanics, as it provides insights into postural strategies and motor control. The data received from analyzing the center of pressure can be viewed in the form of a stabilogram (where each axis represents a direction) or as a time series. The work presented calculated COP using formulas assuming perpendicular forces acting on a force plate. The calculation methodology was validated in previous studies [30, 31] which ensured consistency in COP determination. Figure 11 shows stabilograms that effectively illustrate COP positioning when a subject assumes stances on different areas of the force plate, including forward stance, rightward stance, leftward stance, and backward stance. Figures 12 and 13 present time series data of displacement in the ML and AP directions. The graphs allow for visualization of the movement of the subject over time while standing on the force plate. The significant difference in peak-to-peak amplitudes between the ML and AP directions (103.15mm and 464.57mm) supports the expected wider stance in the AP direction aligning with the COP dynamics. Custom MATLAB code was created for the purpose of analyzing force readings from the force plate. Figure 14 shows the graph of calculated body weight percentages based on left and right limb loading and depicts fluctuations in force loading around the expected mean of 50% of the subject's body weight. The results are consistent with biomechanical principles Winter [35] as they reveal the characteristic loading and unloading patterns during quiet stance. It is also important to note that there is slight variability in the results shown due to the intrinsic variability in the load cell readings due to the nature of their

manufacturing (+-2% full scale error). Since each load cell is susceptible to this amount of error, it is logical to conclude that the modest discrepancies from the projected 50% bodyweight result from the total reading from the scale, since the calculation is based on a constant fixed reported weight. The small variances due to this can cause the force readings to slightly overshoot and undershoot, but overall the trend stays within a reasonable range (less than 5% deviation). The integrity of the biomechanical assumptions that underpin the research is maintained because this variance does not considerably reduce the usefulness of the data for differentiating loading relationships.

The need for emphasizing the use of graphical representation for these analyses is because the visual nature of the graphs facilitate intuitive interpretation and comparison of trends in displacement in both the AP and ML directions. Transforming large amounts of numerical data output by the technology used into more accessible formats allows for a quicker way to identify potential patterns or anomalies that may exist pertaining to postural stability.

The Xsens Awinda system was used to monitor COM and body segment position data of a subject under different visual conditions. As shown in Figures 16 and 17 testing was done with the subject having their eyes opened and eyes closed, with a transition between the conditions occurring at the midpoint of the duration of the trial. During the Eyes Opened condition, the COM exhibited a smaller amplitude range, indicating a more stable stance. During the Eyes Closed condition, the amplitude range increased, reflecting greater variability in the COM position. The observation aligns with previous research showing that visual input influences postural control mechanisms. MATLAB code was developed to perform statistical analysis on COM data captured by the Xsens Awinda system. The standard deviation, variance, range, and mean absolute deviation were computed for the eyes open and eyes closed conditions. The increased dispersion and deviation from the COM during the eyes closed conditions suggest a greater magnitude of postural sway. This reflects the reliance on visual cues for maintaining stability.

A correlation analysis was conducted between the load cell signals from the force plate and the Xsens Awinda system. For this analysis to be done, the sampling frequency from the Xsens

Awinda was first downsampled from 60 Hz to 10 Hz. The correlation value of 0.71 between the two systems was high, indicating that synchronization of both data acquisition systems is strongly correlated. The synchronization is important for enabling simultaneous data collection. The ability to integrate the systems highlights that people using the system can capture real-time data on COP from the force plate along with Xsens Awinda IMU data with minimal delay as well, as seen by the small lag value of 68 milliseconds. This is negligible when pertaining to the data being collected particularly since the system is to be used for conducting trials over extended periods of time.

In past research involving dynamic visual environments, COP was typically the only measurement taken, and this was done under the assumption that subject's responses were purely due to the optic field. However, COP dynamics are an aggregate of actions of different body segments. According to Keshner et al [29], the results of the studies conducted suggest that relying purely on base of support measurements taken might obscure more intricate processes that come into play when responding to a dynamic visual environment. Despite the overarching goal of having the ability to maintain a vertical stance, postural controllers might have motion boundaries for each body segment, rather than being governed only by visual vertical perception. The information shows the responses of body segments in maintaining posture while being exposed to visual stimuli. This strengthens the need for the project presented in this thesis, as it validates a system that can introduce visual stimuli exposure and provide information about body segments in order to analyze postural control.

Spectral analysis of body sway has been used in the evaluation of postural control. Examining body sway in the frequency domain can deliver information on usage of postural strategies. Lower frequency bands are associated with visual regulation, while medium frequency bands are associated with vestibular and somatosensory regulation, and high frequency bands are associated with proprioceptive regulation [40]. Graphs in Figure 31 show comparable shape to the data acquired from the PSD analysis conducted in this thesis.
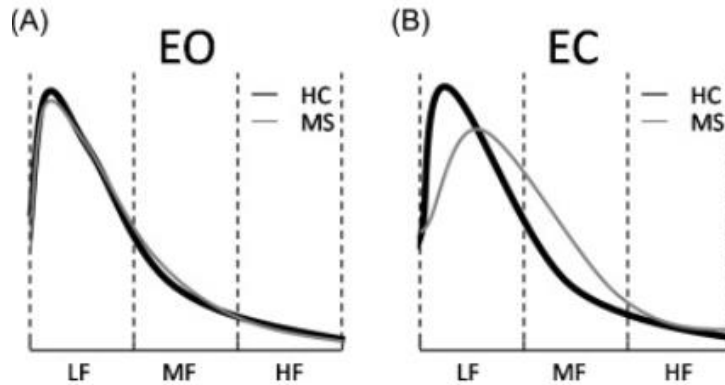
Figure 31: COP power spectrum distribution shift in the ML direction for three frequency bands (eyes open (EO) (A) and the eyes closed (EC) (B) conditions) from Kanekar et al. [40].

For all PSD analysis, it is important to note that selection of window length is somewhat arbitrary. Longer window lengths have much finer frequency resolutions, but at the expense of easy influence of transients. Shorter window lengths lose spectral resolution on the x-axis, but the signals received are less likely to be influenced by noise from transients. This can be seen when comparing Figure 27 and Figure 28, which examine the same set of vector data. Figure 28, which is the graph with window length that is a third of the data length shows a more consistent separation, although there is more ringing in the signal than in Figure 27. However, it is important to note that both graphs show relatively consistent separations between the eyes opened and eyes closed conditions, with a more notable separation in the 0-2.5 Hz frequencies. This is consistent with previous research in that vision plays a greater role in postural control and low to mid frequency bands. More sway is expected when the eyes are closed than when the eyes are opened due to lack of visual input. In theory, the separation when testing a healthy subject and comparing to a patient that suffers from impairment could be analyzed, and one would expect to see a much larger difference in the eyes opened to eyes closed.

In this thesis, the relationship between postural control, frequency-dependent sway, and biomechanical responses in leg and trunk segments during various testing conditions was investigated. The results of analysis of leg and trunk movements allow for a user of the gamification system to be able to explore frequency specific variations. Figure 27 shows the difference between the eyes opened condition and the eyes closed condition for the COM in the

ML direction. The graph shows a notable separation in the low to mid frequency band which is where vision plays a greater role in postural control.

For the two segment body sway analysis, the assumption was made that the trunk and leg segments exclude the knee. The assumption is made based on the fact shown by previous research that knee joints remain relatively stationary during AP sway motion [46]. The angles of the trunk and leg segments in the AP and ML directions relative to the vertical were determined using Xsens IMU markers located on the ankles, the head of the pelvis, and the shoulders. A series of tests were conducted on one subject under eight different conditions. Each trial consisted of a direction of tilt, either forward tilt, rightward tilt, backward tilt, or leftward tilt. Each trial consisted of either an eyes open condition or a VR rolling visual condition (as referenced in Table 10). Figure 30 shows several subplots of data collected pertaining to the ML direction for leg segment angles and trunk segment angles. For each trial, a graph of the leg versus trunk segment PSD plot was created. The y-axis represents power/frequency (dB/Hz) and the x-axis represents frequency in Hertz. In those graphs, Data Column 1 represents leg segments, and Data Column 2 represents trunk segments.

A notable observation shown from these trials was that the power of the leg segment data (represented in blue) was generally consistently higher in power than the trunk segment data (represented in orange). For the trials conducted on this subject, this pattern was seen especially at frequencies of 1.5 Hz and above. In addition to this, the separation between leg and trunk segments are visibly more pronounced at higher frequencies. The biomechanics that are referred to in this context relate to the ease of rapidly moving a heavy object. In this case, the head and the trunk are considered to be the heavy object, also known as the HAT (Head, Arms, and Trunk). This is used to refer to the upper part of the body, as this part of the body is often considered as a single unit in biomechanical studies as it accounts for approximately two-thirds of the body's total weight. From a postural control perspective, the human brain aims to keep the trunk and head of the body upright. The brain can facilitate this task more easily at higher frequencies if the trunk does not "ride" on top of the moving legs. Rather, the legs become free to shift under a less mobile trunk. This interpretation is supported by the data and is demonstrated by the PSD graphs. The pattern of leg segment frequencies being generally higher

than the trunk segment frequencies suggests that the legs are moving more freely under the trunk. The larger separations in the leg and trunk segment data at frequencies above 1.5 Hz also further highlights the difference in low-frequency and high-frequency sway. At lower frequencies, the trunk may be more likely to "ride" on top of the legs, thus indicating that it is possible for a different postural strategy to be used, while at higher frequencies, the legs can appear to move more freely under a less mobile trunk. The distinction is important for understanding the biomechanics of postural control, as it could highlight the role of these different body segments and how their dynamics change depending on different frequencies.

For the rightward tilt, leftward tilt, and backward tilt conditions, it can also be noted in Figure 30 (graphs C-H) that the visual roll condition graphs show higher power overall than the eyes opened, no VR conditions. This observation holds true for both the leg segments and the trunk segments. An exception is seen in graphs A and B for the forward tilt condition, where the power does not significantly decrease with visual roll, possibly due to the subject's familiarity with the forward tilt position. However, this anomalous result should be considered with caution as it deviates from the general trend observed in the other conditions. The results further corroborate the fact that visual stimulus has influence on postural sway, as higher power can be indicative of more variability in sway (inherently allowing for information output by the gamification system to show that a subject may be experiencing less stability).

Overall, the methods used in this thesis to collect and present data show that the gamification system is able to detect changes in postural sway, which is vital to being able to conduct larger group studies. The system was proven to be able to detect differences in postural sway in using different metrics of COP, COM, and body segment analysis. It is important to note that testing and gathering the balance data for this thesis was only conducted on one subject, but the processes developed in the thesis could be adapted to large scale human trials.

9.0 CONCLUSION

The integration of VR, Xsens Awinda, the force plate, and the BASE system offers a robust gamification system for assessing balance and spatial orientation abilities in controlled experimental settings. The validation of the system fortifies its credibility as a resourceful tool for facilitating more extensive studies, ensuring safety, providing a structured method of protocol for use, and enabling extraction and presentation of data in a meaningful manner. The versatility of the system can be leveraged to have a subject perform tasks across a wide range of angles, both statically and dynamically. This is crucial for balance studies as it emulates a more organic setting that is free from many limitations of other previous research that has been conducted, including fixed viewing directions or the requirement of being in a seated or supine position. The selection of relevant data across all of the subsystems is an essential component, as it ensures the analysis is concentrated on data significant to the relevant biomechanical processes being studied, preventing an overload of information that could obscure the importance of findings. The results of using VR in order to simultaneously conduct SVV tests while using the BASE can provide data that could be used to analyze potential vestibular dysfunction. The system's sensitivity to visual conditions and its ability to capture both body segment, COM, and COP dynamics in real-time provide valuable insights into postural control mechanisms and sway characteristics. The work presented in this thesis demonstrates the potential for use of this system in biomechanical analysis, medical rehabilitation, and balance training.

10.0 FUTURE WORK

The gamification system has shown promise for the potential ability to be utilized for balance studies. Future work should include larger scale group studies. Balance ability can vary from subject to subject, including hip and ankle strategies that they resort to depending on different frequencies of platform perturbations. Visual conditions on these strategies could be investigated as well. Different visual scenarios could be created and displayed in VR, including more interactive games or other spatial awareness tests geared toward clinical use. The Xsens system's ability to analyze various aspects of body segments could also be further explored. The data from power spectral analysis done in this thesis has shown that the technology is capable of providing data that can be used to analyze body segment behavior. Cophase analysis of segments could be further looked into in order to provide valuable insights on balance control mechanisms that differentiate healthy subjects to those with impairments, such as multiple sclerosis. Based on the significant potential that the system demonstrates, it is of hope that it could be utilized further to expand understanding and capabilities of balance studies, and be used to develop more effective and personalized training and rehabilitation programs.

ACKNOWLEDGEMENTS

CITATIONS

[1] Clément G, Moudy SC, Macaulay TR, Bishop MO and Wood SJ (2022), Mission-critical tasks for assessing risks from vestibular and sensorimotor adaptation during space exploration. Front.Physiol. 13:1029161. doi: 10.3389/fphys.2022.1029161

[2] T. R. Macaulay, B. T. Peters, S. J. Wood, G. R. Clément, L. Oddsson, and J. J. Bloomberg, "Developing Proprioceptive Countermeasures to Mitigate Postural and Locomotor Control Deficits After Long-Duration Spaceflight," Frontiers in Systems Neuroscience, vol. 15, 2021. [Online]. Available: https://www.frontiersin.org/articles/10.3389/fnsys.2021.658985. doi: 10.3389/fnsys.2021.658985. ISSN: 1662-5137.

[3] Winter, C., Kern, F., Gall, D. et al. Immersive virtual reality during gait rehabilitation increases walking speed and motivation: a usability evaluation with healthy participants and patients with multiple sclerosis and stroke. J NeuroEngineering Rehabilitation 18, 68 (2021). https://doi.org/10.1186/s12984-021-00848-w

[4] Steven Phu, Sara Vogrin, Ahmed Al Saedi & Gustavo Duque (2019) Balance training using virtual reality improves balance and physical performance in older adults at high risk of falls, Clinical Interventions in Aging, , 1567-1577, DOI: 10.2147/CIA.S220890

[5] A. González, M. Hayashibe, V. Bonnet, and P. Fraisse, "Whole Body Center of Mass Estimation with Portable Sensors: Using the Statically Equivalent Serial Chain and a Kinect," Sensors, vol. 14, pp. 16955-16971, Sep. 2014. doi: 10.3390/s140916955. Available: www.mdpi.com/journal/sensors. ISSN: 1424-8220. Open Access.

[6] Lehmann JF, Boswell S, Price R, et al. Quantitative evaluation of sway as an indicator of functional balance in post-traumatic brain injury. Archives of Physical Medicine and Rehabilitation. 1990 Nov;71(12):955-962. PMID: 2241541.

[7] Lord SR, Murray SM, Chapman K, Munro B, Tiedemann A. Sit-to-stand performance depends on sensation, speed, balance, and psychological status in addition to strength in older people. J Gerontol A Biol Sci Med Sci. 2002 Aug;57(8):M539-43. doi: 10.1093/gerona/57.8.m539. PMID: 12145369.

[8] Moe-Nilssen, R., & Helbostad, J. L. (2005). Interstride trunk acceleration variability but not step width variability can differentiate between fit and frail older adults. *Gait & Posture*, 21(2), 164-170. https://doi.org/10.1016/j.gaitpost.2004.01.013

[9] Piirtola M, Era P. Force platform measurements as predictors of falls among older people - a review. Gerontology. 2006;52(1):1-16. doi: 10.1159/000089820. PMID: 16439819.

[10] Dvorkin, A.Y., Kenyon, R.V. & Keshner, E.A. Effects of roll visual motion on online control of arm movement: reaching within a dynamic virtual environment. Exp Brain Res 193, 95–107 (2009). https://doi.org/10.1007/s00221-008-1598-z

[11] Tanahashi, S., Ujike, H., Kozawa, R. et al. Effects of visually simulated roll motion on vection and postural stabilization. J NeuroEngineering Rehabil 4, 39 (2007). https://doi.org/10.1186/1743-0003-4-39

[12] Lubeck, A.J.A., Bos, J.E. & Stins, J.F. Framing visual roll-motion affects postural sway and the subjective visual vertical. *Atten Percept Psychophys* 78, 2612–2620 (2016). https://doi.org/10.3758/s13414-016-1150-3

[13] Wang, Y., Du, B., Wei, Y., & So, R. H. Y. (2021). Visually Induced Roll Circular Vection: Do Effects of Stimulation Velocity Differ for Supine and Upright Participants? Frontiers in Virtual Reality, 2, 611214. [Online]. Available: https://www.frontiersin.org/articles/10.3389/frvir.2021.611214 doi: 10.3389/frvir.2021.611214. ISSN: 2673-4192.

[14] B. K. Ward, C. J. Bockisch, N. Caramia, G. Bertolini, and A. A. Tarnutzer, "Gravity dependence of the effect of optokinetic stimulation on the subjective visual vertical," Journal of Neurophysiology, vol. 117, no. 5, pp. 1891-1897, May 2017. doi: 10.1152/jn.00303.2016. Available: https://doi.org/10.1152/jn.00303.2016.

[15] Cleworth, T.W.; Allum, J.H.J.; Nielsen, E.I.; Carpenter, M.G. The Effect of Roll Circular Vection on Roll Tilt Postural Responses and Roll Subjective Postural Horizontal of Healthy Normal Subjects. Brain Sci. 2023, 13, 1502. https://doi.org/ 10.3390/brainsci13111502

[16] King, A. C., Patton, J., Dutt-Mazumder, A., & Newell, K. M. (2020). Center-of-pressure dynamics of upright standing as a function of sloped surfaces and vision. *Neuroscience Letters*, 737, 135334. https://doi.org/10.1016/j.neulet.2020.135334

[17] Goldie PA, Bach TM, Evans OM. Force platform measures for evaluating postural control: reliability and validity. Archives of Physical Medicine and Rehabilitation. 1989 Jul;70(7):510-517. PMID: 2742465.

[18] Hasan, S. S., Robin, D. W., Szurkus, D. C., Ashmead, D. H., Peterson, S. W., & Shiavi, R. G. (1996). Simultaneous measurement of body center of pressure and center of gravity during upright stance. Part I: Methods. *Gait & Posture, 4*(1), 1-10. https://doi.org/10.1016/0966-6362(95)01030-0

[19] Newson JJ, Thiagarajan TC. EEG Frequency Bands in Psychiatric Disorders: A Review of Resting State Studies. Front Hum Neurosci. 2019 Jan 9;12:521. doi: 10.3389/fnhum.2018.00521. PMID: 30687041; PMCID: PMC6333694.

[20] Mauritz KH, Dichgans J, Hufschmidt A. Quantitative analysis of stance in late cortical cerebellar atrophy of the anterior lobe and other forms of cerebellar ataxia. Brain. 1979 Sep;102(3):461-82. doi: 10.1093/brain/102.3.461. PMID: 315255.

[21] Cherng, R.-J., Lee, H.-Y., & Su, F.-C. (2003). Frequency spectral characteristics of standing balance in children and young adults. *Medical Engineering & Physics, 25*(6), 509-515. https://doi.org/10.1016/S1350-4533(03)00049-3

[22] Horak, Fay B., and Lewis M. Nashner. "Central programming of postural movements: adaptation to altered support-surface configurations." *Journal of neurophysiology* 55, no. 6 (1986): 1369-1381.

[23] Horak, F. B. "Handbook of physiology, Section 12: Exercise: Regulation and integration of multiple systems." *(No Title)* (1996): 255.

[24] McCollum, Gin, and Todd K. Leen. "Form and exploration of mechanical stability limits in erect stance." *Journal of Motor Behavior* 21, no. 3 (1989): 225-244

[25] Winters, Jack M., and Patrick E. Crago, eds. *Biomechanics and neural control of posture and movement*. Springer Science & Business Media, 2012.

[26] Mergner, T., W. Huber, and W. Becker. "Vestibular-neck interaction and transformation of sensory coordinates." *Journal of Vestibular Research* 7, no. 4 (1997): 347-365.

[27] Zhang, Y., Kiemel, T., & Jeka, J. (2007). The influence of sensory information on two-component coordination during quiet stance. *Gait & Posture, 26*(2), 263-271. https://doi.org/10.1016/j.gaitpost.2006.09.007

[28] Creath R, Kiemel T, Horak F, Jeka JJ. The role of vestibular and somatosensory systems in intersegmental control of upright stance. J Vestib Res. 2008;18(1):39-49. PMID: 18776597; PMCID: PMC2938746.

[29] Keshner, E.A., and Kenyon, R.V. 2000. "The Influence of an Immersive Virtual Environment on the Segmental Organization of Postural Stabilizing Responses." *Journal of Vestibular Research* 10: 207-219. ISSN 0957-4271. IOS Press.

[30] Bartlett, H. L., Ting, L. H., & Bingham, J. T. (2013). Accuracy of force and center of pressure measures of the Wii Balance Board. *Gait & Posture*, 38(4), 305-3061

[31] M. A. G. Fauzi, H. Mukhtar and D. Rahmawati, "Assessment of Postural Stability Using an Affordable and Simple Force Platform," 2021 IEEE 7th International Conference on Smart Instrumentation, Measurement and Applications (ICSIMA), Bandung, Indonesia, 2021, pp. 252-256, doi: 10.1109/ICSIMA50015.2021.9526294.

[32] Bauer C, Gröger I, Rupprecht R, Meichtry A, Tibesku CO, Gaßmann K-G. Reliability analysis of time series force plate data of community dwelling older adults. Arch Gerontol Geriatr. 2010;51(3):100–5.

[33] Patti A, Bianco A, Şahin N, Sekulic D, Paoli A, Iovane A, Messina G, Gagey PM, Palma A. Postural control and balance in a cohort of healthy people living in Europe: An observational study. Medicine (Baltimore). 2018 Dec;97(52):e13835. doi: 10.1097/MD.0000000000013835. PMID: 30593180; PMCID: PMC6314740.

[34] T. E. Prieto, J. B. Myklebust and B. M. Myklebust, "Characterization and modeling of postural steadiness in the elderly: a review," in *IEEE Transactions on Rehabilitation Engineering*, vol. 1, no. 1, pp. 26-34, March 1993, doi: 10.1109/86.242405.

[35] Winter, D. A. (1995). Human balance and posture control during standing and walking. Gait & Posture, 3(4), 193-214.

[36] Whitney, David, and Patrick Cavanagh. "Motion distorts visual space: shifting the perceived position of remote stationary objects." *Nature neuroscience* 3, no. 9 (2000): 954-959.

[37] Nishida, Shin'ya, and Alan Johnston. "Influence of motion signals on the perceived position of spatial pattern." *Nature* 397, no. 6720 (1999): 610-612.

[38] Brandt, Th, M. Dieterich, and A. Danek. "Vestibular cortex lesions affect the perception of verticality." *Annals of Neurology: Official Journal of the American Neurological Association and the Child Neurology Society* 35, no. 4 (1994): 403-412.

[39] Dichgans, J., Brandt, T. (1978). Visual-Vestibular Interaction: Effects on Self-Motion Perception and Postural Control. In: Held, R., Leibowitz, H.W., Teuber, HL. (eds) Perception. Handbook of Sensory Physiology, vol 8. Springer, Berlin, Heidelberg. https://doi.org/10.1007/978-3-642-46354-9_25

[40] Kanekar, N., Lee, Y-J., & Aruin, A. S. (2014). Frequency analysis approach to study balance control in individuals with multiple sclerosis. Journal of Neuroscience Methods, 222, 91-96. https://doi.org/10.1016/j.jneumeth.2013.10.020

[41] Tanahashi, S., Ujike, H., & Ukai, K. (2012). Visual rotation axis and body position relative to the gravitational direction: Effects on circular vection. *i-Perception*, 3, 804–819. https://doi.org/10.1068/i0479

[42] Pavan, Theo Zeferino, Martha Funabashi, José Ailton Oliveira Carneiro, Taiza Elaine Grespan dos Santos Pontelli, Walfred Tedeschi, José Fernando Colafêmina, and Antonio Adilton Olivera Carneiro. "Software for subjective visual vertical assessment: an observational cross-sectional study." *Brazilian journal of otorhinolaryngology* 78, no. 5 (2012): 51-58.

[43] Böhmer, Andreas, and Fred Mast. "Assessing otolith function by the subjective visual vertical." *Annals of the New York Academy of Sciences* 871, no. 1 (1999): 221-231.

[44] Kumagami, Hidetaka, Yuzuru Saino, Akiko Baba, Daisuke Fujiyama, Kenji Takasaki, and Haruo Takahashi. "Subjective visual vertical test in patients with chronic dizziness without abnormal findings in routine vestibular function tests." *Acta Oto-Laryngologica* 129, no. sup562 (2009): 46-49.

[45] Landau, Mark E., and Kristen C. Barner. "Vestibulocochlear nerve." In *Seminars in neurology*, vol. 29, no. 01, pp. 066-073. © Thieme Medical Publishers, 2009.

[46] Alexandrov AV, Frolov AA, Massion J. Biomechanical analysis of movement strategies in human forward trunk bending. I. Modeling.

Biol Cybern 2001;84(6):425–34.

[47] Berra K (2004) Virtual rehabilitation: dream or reality? Clin Invest Med 29:187-192

[48] B. Quinlivan, J. S. Butler, I. Beiser, L. Williams, E. McGovern, S. O'Riordan, M. Hutchinson, and R. B. Reilly, "Application of virtual reality head mounted display for investigation of movement: a novel effect of orientation of attention," Journal of Neural Engineering, vol. 13, no. 5, Aug. 2016, Art. no. 056006. [Online]. Available: https://doi.org/10.1088/1741-2560/13/5/056006

[49] D. A. E. Bolton, "The role of the cerebral cortex in postural responses to externally induced perturbations," Neuroscience & Biobehavioral Reviews, vol. 57, pp. 142-155, 2015. [Online]. Available: https://doi.org/10.1016/j.neubiorev.2015.08.014

[50] Mao Y, Chen P, Li L, Huang D. Virtual reality training improves balance function. Neural Regen Res. 2014 Sep 1;9(17):1628-34. doi: 10.4103/1673-5374.141795. PMID: 25368651; PMCID: PMC4211206.

[51] Huang CW, Sue PD, Abbod MF, Jiang BC, Shieh JS. Measuring center of pressure signals to quantify human balance using multivariate multiscale entropy by designing a force platform. Sensors (Basel). 2013 Aug 8;13(8):10151-66. doi: 10.3390/s130810151. PMID: 23966184; PMCID: PMC3812597.

[52] Blanchet, M., Prince, F., & Messier, J. (2018). Development of postural stability limits: Anteroposterior and mediolateral postural adjustment mechanisms do not follow the same maturation process. Human Movement Science. https://doi.org/10.1016/j.humov.2018.11.016

[53] Smith, J.O. (2011). Spectral Audio Signal Processing. Retrieved from http://ccrma.stanford.edu/~jos/sasp/.

APPENDIX

Appendix A) Arduino code for obtaining calibration factors of S-type load cell

```
#include "HX711.h" //This library can be obtained here http://librarymanager/All#Avia_HX711

#define LOADCELL_DOUT_PIN  47
#define LOADCELL_SCK_PIN  45

HX711 scale;

float calibration_factor = -22700;

void setup() {
  Serial.begin(9600);
  Serial.println("HX711 calibration sketch");
  Serial.println("Remove all weight from scale");
  Serial.println("After readings begin, place known weight on scale");
  Serial.println("Press + or a to increase calibration factor");
  Serial.println("Press - or z to decrease calibration factor");

  scale.begin(LOADCELL_DOUT_PIN, LOADCELL_SCK_PIN);
  scale.set_scale();
  scale.tare(); //Reset scale to 0 for tare

  long zero_factor = scale.read_average(); //Obtaining baseline reading
  Serial.print("Zero factor: "); //
  Serial.println(zero_factor);
}

void loop() {

  scale.set_scale(calibration_factor); //Use to adjust baseline factor

  Serial.print("Reading: ");
  Serial.print(scale.get_units(), 1);
  Serial.print("kg");
  Serial.print(" calibration_factor: ");
  Serial.print(calibration_factor);
  Serial.println();

  if(Serial.available())
  {
    char temp = Serial.read();
    if(temp == '+' || temp == 'a')
      calibration_factor += 10;
    else if(temp == '-' || temp == 'z')
      calibration_factor -= 10;
  }
}
```

Appendix B) Arduino Code to show scale outputs

```cpp
#include "HX711.h"          // This library can be obtained here http://librarymanager/All#Avia_HX711
//calibration values
//-21350 for sensor 1
//-20850 for sensor 2
//-22700 for sensor 3
//-22700 for sensor 4
#define Sensor1_DOUT_PIN 50
#define Sensor1_SCK_PIN 48

#define Sensor2_DOUT_PIN 46
#define Sensor2_SCK_PIN 44

#define Sensor3_DOUT_PIN 51
#define Sensor3_SCK_PIN 49

#define Sensor4_DOUT_PIN 47
#define Sensor4_SCK_PIN 45

HX711 scale_sensor1;
HX711 scale_sensor2;
HX711 scale_sensor3;
HX711 scale_sensor4;

void setup() {
  Serial.begin(9600);
  Serial.println("HX711 scale demo");

  scale_sensor1.begin(Sensor1_DOUT_PIN, Sensor1_SCK_PIN);
  scale_sensor2.begin(Sensor2_DOUT_PIN, Sensor2_SCK_PIN);
  scale_sensor3.begin(Sensor3_DOUT_PIN, Sensor3_SCK_PIN);
  scale_sensor4.begin(Sensor4_DOUT_PIN, Sensor4_SCK_PIN);

  scale_sensor1.set_scale(-21350); //calibtraion value for sensor 1
  scale_sensor2.set_scale(-20850); //calibration value for sensor 2
  scale_sensor3.set_scale(-22700); //calibration value for sensor 3
  scale_sensor4.set_scale(-22700); //calibration value for sensor 4

  scale_sensor1.tare();
  scale_sensor2.tare();
  scale_sensor3.tare();
  scale_sensor4.tare();


  Serial.println("Readings:");
}

void loop() {
  Serial.print("Reading: ");
  Serial.print(scale_sensor1.get_units(), 1); //scale.get_units() returns a float
  Serial.print(",");
  Serial.print(scale_sensor2.get_units(), 1); //scale.get_units() returns a float
  Serial.print(",");
  Serial.print(scale_sensor3.get_units(), 1); //scale.get_units() returns a float
  Serial.print(",");
  Serial.print(scale_sensor4.get_units(), 1); //scale.get_units() returns a float
  Serial.print(" kg");
  Serial.println();
}
```

Appendix C) MATLAB code to calculate and graph fluctuations in movement based on bodyweight

```matlab
% Input the subject's body weight in kg
bodyWeight = 62; % input variable body weight dependent on subject
% Read the data from Excel file
data = xlsread('FluctuatingGraph.xlsx');
% Sampled at 10 HZ
time = (0:length(data)-1)/10;
% Forces are already in kg, convert to body weight percent
leftForcePercent = (data(:,1) / bodyWeight) * 100;
rightForcePercent = (data(:,2) / bodyWeight) * 100;
% Create the plot
figure;
plot(time, leftForcePercent, 'b');
hold on;
plot(time, rightForcePercent, 'r');
xlabel('Time (s)');
ylabel('Body Weight (%)');
legend('Left Force', 'Right Force');
title('Body Weight Percent vs Time');
grid on;
% Load data
data_open = xlsread('Eyesopened.xlsx', 'B:B');
data_closed = xlsread('Eyesclosed.xlsx', 'B:B');
% Calculate measurements
std_dev_open = std(data_open);
std_dev_closed = std(data_closed);
variance_open = var(data_open);
variance_closed = var(data_closed);
range_open = range(data_open);
```

```matlab
range_closed = range(data_closed);

mad_open = mad(data_open);

mad_closed = mad(data_closed);

% Display results

disp(['Standard deviation (Eyes opened): ', num2str(std_dev_open)])

disp(['Standard deviation (Eyes closed): ', num2str(std_dev_closed)])

disp(['Variance (Eyes opened): ', num2str(variance_open)])

disp(['Variance (Eyes closed): ', num2str(variance_closed)])

disp(['Range (Eyes opened): ', num2str(range_open)])

disp(['Range (Eyes closed): ', num2str(range_closed)])

disp(['Mean absolute deviation (Eyes opened): ', num2str(mad_open)])

disp(['Mean absolute deviation (Eyes closed): ', num2str(mad_closed)])

% Create figure for the bar charts

figure;

% Create bar chart for standard deviation

subplot(2,3,1);

bar([std_dev_open, std_dev_closed]);

title('Standard Deviation');

set(gca, 'XTickLabel', {'Eyes Opened', 'Eyes Closed'});

% Create bar chart for variance

subplot(2,3,2);

bar([variance_open, variance_closed]);

title('Variance');

set(gca, 'XTickLabel', {'Eyes Opened', 'Eyes Closed'});

% Create bar chart for range

subplot(2,3,3);

bar([range_open, range_closed]);

title('Range');

set(gca, 'XTickLabel', {'Eyes Opened', 'Eyes Closed'});

% Create bar chart for mean absolute deviation

subplot(2,3,4);
```

bar([mad_open, mad_closed]);

title('Mean Absolute Deviation');

set(gca, 'XTickLabel', {'Eyes Opened', 'Eyes Closed'});

% Adjust layout

set(gcf, 'Position', [100, 100, 800, 600]);

Appendix D) MATLAB code to compute and plot cross correlation functions to

```matlab
% Specify Excel file name
filename = 'downsampling test.xlsx';
% Read the data from the Excel file
data = xlsread(filename);
% Extract data
A = data(:,1);
B = data(:,2);
% Compute the normalized cross-correlation
C = xcorr(A, B, 'coeff');
% Create a time vector
lags = -(length(A)-1):(length(B)-1);
% Create figure
figure;
% Plot cross-correlation function
plot(lags, C);
% Graph titles
title('Cross-Correlation Function');
xlabel('Lag');
ylabel('Correlation');
% Display the figure
grid on;
```

Appendix E) MATLAB code to calculate body segment angles

```matlab
% Load data from Excel file
filename = 'clean.xlsx';
data = xlsread(filename);
% First column is the x-axis data and the second column is the y-axis
y_data = data(:, 1);
x_data = data(:, 2);
% Calculate angle using the atan2d function
angle_data = atan2d(y_data, x_data);
% Write angle data to a new Excel file
output_filename = 'trl.xlsx'; % input the output file name
xlswrite(output_filename, angle_data);
```

Appendix F) MATLAB code created for PSD calculations

```matlab
% Load data from Excel file
filename = '004angles.xlsx'; % replace with your file name
data1 = xlsread(filename, 'A:A'); % reads data, first column
data2 = xlsread(filename, 'B:B'); % reads data, second column
% Performing Power Spectral Density estimation using Welch's method for both data columns
[pxx1, freq1] = pwelch(data1,hanning(length(data1)*.3),[],[0:.1:5],60);
[pxx2, freq2] = pwelch(data2,hanning(length(data2)*.3),[],[0:.1:5],60);
% Plotting the power spectral density for both data columns
figure;
plot(freq1,10*log10(pxx1))
hold on
plot(freq2,10*log10(pxx2))
title('Power Spectral Density of data')
xlabel('Frequency (Hz)')
ylabel('Power/Frequency (dB/Hz)')
legend('Data Column 1','Data Column 2')
```

Appendix G) MATLAB code created for PSD calculations

Code for bar graph from VS Code

```
using System.Collections;
using System.Collections.Generic;
using TMPro;
using UnityEngine;
public class BarGraph : MonoBehaviour
{
    [SerializeField] GameObject barObj;
    [SerializeField] GameObject barValueObj;
    [SerializeField] float maxValue = 180.0f;
    [SerializeField] float maxBarSize = 10.0f;
    [SerializeField] float vertSpacing;
    [SerializeField] float startVert;
    [Tooltip("Uses this offset if bar's position is too close")]
    [SerializeField] float minValueOffsetFromMidline;
    private RectTransform[] bars;
    public void GenerateGraph(List<float> values)
    {
        bars = new RectTransform[values.Count];
        for (int i = 0; i < values.Count; i++)
        {
            values[i] = (int)values[i]; // ROUND TO INTEGER
            bars[i] = Instantiate(barObj, Vector3.zero, Quaternion.identity,
this.transform).GetComponent<RectTransform>();
            bars[i].localPosition = Vector3.up * ((i) * vertSpacing + startVert);
            // Converts bar val to bar length
            float l = Mathf.InverseLerp(0.0f, maxValue, Mathf.Abs(values[i]));
            bars[i].localScale = new Vector3(l * maxBarSize, 1, 1);
```

```
        float offset = bars[i].rect.width * bars[i].localScale.x / 2.0f; // We need to offset our bar
locally by its rect
        bars[i].localPosition += Vector3.right * offset * ((values[i] < 0.0f) ? -1.0f : 1.0f);
        // Visualize bar's value on correct side
        RectTransform valueObject = Instantiate(barValueObj,
this.transform).GetComponent<RectTransform>();
        valueObject.localPosition = new Vector3(
          (Mathf.Abs(bars[i].localPosition.x) < minValueOffsetFromMidline) ?
minValueOffsetFromMidline * ((values[i] < 0.0f) ? -1.0f : 1.0f) : bars[i].localPosition.x,
          bars[i].localPosition.y,
          0.0f);
        valueObject.GetComponentInChildren<TextMeshProUGUI>().text =
values[i].ToString();
      }
    }
}
```

Sphere Rotation

```
using System.Collections;
using System.Collections.Generic;
using UnityEngine;

public class createSpheres : MonoBehaviour
{
    [SerializeField] private int sphereNum;

    [SerializeField] private GameObject spherePrimitive;

    [SerializeField] public int speedOfRotation;


    // Update is called once per frame
    void Update()
    {
```

```
    this.transform.localEulerAngles = new Vector3(0.0f, 0.0f, this.transform.localEulerAngles.z
+ speedOfRotation * Time.deltaTime);
    //this.transform.RotateAround(Vector3.zero, Vector3.forward, speedOfRotation *
Time.deltaTime);
  }
}
```

VS Code for rotating line

```
using System.Collections.Generic;
using UnityEngine;
using UnityEngine.InputSystem;
using UnityEngine.UI;
using UnityEngine.XR.Interaction.Toolkit;
//Rotates the line with input and calculates the score
public class rotateLine : MonoBehaviour
{
   [SerializeField] float speed;
   [SerializeField] int trials;
   [SerializeField] Canvas canvas;
   [SerializeField] BarGraph barGraph;
   [SerializeField] private InputActionReference rotateLineInputReferenceLeftTrigger;
   [SerializeField] private InputActionReference rotateLineInputReferenceRightTrigger;
   [SerializeField] private InputActionReference instructorContinueTrigger; // Continue to the
next round
   [SerializeField] private InputActionReference instructorResetTrigger;    // Completely reset
the game
   [SerializeField] private MiniSceneLoader miniSceneLoader;
   [Space]
   [SerializeField] int currentRound = 0;
   private ActionBasedController controller;
   private XRBaseInteractor interactor;
```

```csharp
private bool entered = false;

private List<float> scores;

private float activationThreshold = 0.2f;

private bool reloadKeyHold = false;

void Awake()

{

    // Initialize controllers

    rotateLineInputReferenceLeftTrigger.action.performed += RotLeftTrigger;

    rotateLineInputReferenceRightTrigger.action.performed += RotRightTrigger;

}

void Start()

{

    CompletelyResetTest();

}

private void Update()

{

    InstructorCommands();

    currentRound = scores.Count;

}

/// <summary>

/// Allows the instructor to continue rounds and reset

/// the test using keyboard keys

/// </summary>

private void InstructorCommands()

{

    Keyboard keyboard = Keyboard.current;

    if (keyboard.enterKey.isPressed ) // Reload scene

    {

        miniSceneLoader.ReloadScene();

    }
```

```
        else if (keyboard.spaceKey.isPressed && reloadKeyHold == false) // Continue to next
round
        {
            SetNextRound();
        }
        reloadKeyHold = keyboard.spaceKey.isPressed;
    }
    private void RotRightTrigger(UnityEngine.InputSystem.InputAction.CallbackContext obj)
    {
        print("Hello");
        if (obj.action.ReadValue<float>() != 0 && !entered)
        {
            this.transform.rotation = this.transform.rotation * Quaternion.Euler(0, 0, speed *
Time.deltaTime);
        }
    }
    private void RotLeftTrigger(UnityEngine.InputSystem.InputAction.CallbackContext obj)
    {
        if (obj.action.ReadValue<float>() != 0 && !entered)
        {
            this.transform.rotation = this.transform.rotation * Quaternion.Euler(0, 0, -speed *
Time.deltaTime);
        }
    }
    /// <summary>
    /// Continues to next round if possible. If not creates a graph that
    /// represents the previous rounds of data
    /// </summary>
    private void SetNextRound()
    {
        // Store current difference of rotation
```

```
        float roundSCore = this.transform.eulerAngles.z;

        if (roundSCore >= 90)

        {

            roundSCore = 180 - roundSCore;

        }

        scores.Add(roundSCore);

        if(scores.Count >= trials)

        {

            // Create bar graph and indicate it is the end of round

            canvas.gameObject.SetActive(true);

            barGraph.GenerateGraph(scores);

        }

        else

        {

            // Reset this line to a random rotation

            float z = Random.Range(0, 360);

            this.transform.localEulerAngles = new Vector3(0, 0, z);

        }

    }

    private void CompletelyResetTest()

    {

        // Set this line to a random rotation

        float z = Random.Range(0, 360);

        this.transform.localEulerAngles = new Vector3(0, 0, z);

        scores = new List<float>();

    }

    private void Score()

    {

        //find the distance from quaternion.zero

        float scoreFinal = this.transform.eulerAngles.z;

        if (scoreFinal >= 90)
```

```
        {
            scoreFinal = 180 - scoreFinal;
        }
        scores.Add(scoreFinal);
        if (scores.Count >= trials)
        {
            //displayGraph();
        }
    }
}
```

Code for rotating speed

```
using System.Collections;
using System.Collections.Generic;
using UnityEngine;
public class rotateSpeed : MonoBehaviour
{
    private int velocity;
    private float angles;
    // Start is called before the first frame update
    void Start()
    {
        velocity = this.GetComponentInParent<createSpheres>().speedOfRotation;
        Vector2 position = new Vector2(transform.position.x, transform.position.y);
        angles = velocity/(Vector2.Distance(position, Vector2.zero));
    }
    // Update called once per frame
    void Update()
    {
        this.transform.RotateAround(Vector3.zero, Vector3.forward, velocity * Time.deltaTime);
    }
}
```